The KCC2 Influence on Neuronal Migration in Ferret Neocortex

by

Francis Tanam Djankpa

Dissertation submitted to the Faculty of the
Neuroscience Graduate Program
Uniformed Services University of the Health Sciences
In partial fulfillment of the requirements for the degree of
Doctor of Philosophy 2017

UNIFORMED SERVICES UNIVERSITY, SCHOOL OF MEDICINE GRADUATE PROGRAMS
Graduate Education Office (A 1045), 4301 Jones Bridge Road, Bethesda, MD 20814

FINAL EXAMINATION/PRIVATE DEFENSE FOR THE DEGREE OF DOCTOR OF PHILOSOPHY
IN THE NEUROSCIENCE GRADUATE PROGRAM

Name of Student: Francis T. Djankpa

Date of Examination: Monday, December 11, 2017
Time: 10:00 AM
Place: B2090

DECISION OF EXAMINATION COMMITTEE MEMBERS:

	PASS	FAIL
[redacted]	✓	
Aviva Symes, PhD DEPARTMENT OF PHARMACOLOGY Committee Chairperson		
[redacted]	✓	
Sharon Juliano, PhD DEPARTMENT OF ANATOMY, PHYSIOLOGY & GENETICS Dissertation Advisor		
[redacted]	✓	
Regina Armstrong, PhD DEPARTMENT OF ANATOMY, PHYSIOLOGY & GENETICS Committee Member		
[redacted]	✓	
Martin Doughty, PhD DEPARTMENT OF ANATOMY, PHYSIOLOGY & GENETICS Committee Member		
[redacted]	✓	
Thomas Flagg, PhD DEPARTMENT OF ANATOMY, PHYSIOLOGY & GENETICS Committee Member		

Gregory P. Mueller, Ph.D., Associate Dean || www.usuhs.mil/graded || graduateprogram@usuhs.edu
Toll Free: 800-772-1747 || Commercial: 301-295-3913 / 9474 || DSN: 295-9474 || Fax: 301-295-6772

UNIFORMED SERVICES UNIVERSITY, SCHOOL OF MEDICINE GRADUATE PROGRAMS
Graduate Education Office (A 1045), 4301 Jones Bridge Road, Bethesda, MD 20814

APPROVAL OF THE DOCTORAL DISSERTATION IN THE NEUROSCIENCE GRADUATE PROGRAM

Title of Dissertation: "The KCC2 Influence on Neuronal Migration in Ferret Neocortex"

Name of Candidate: Francis T. Djankpa
Doctor of Philosophy
December 11, 2017

DISSERTATION AND ABSTRACT APPROVED:

DATE:

[redacted]
2/1/18
Aviva Symes, PhD
DEPARTMENT OF PHARMACOLOGY
Committee Chairperson

[redacted]
12/11/2017
Sharon Juliano, PhD
DEPARTMENT OF ANATOMY, PHYSIOLOGY & GENETICS
Dissertation Advisor

[redacted]
12/11/2017
Regina Armstrong, PhD
DEPARTMENT OF ANATOMY, PHYSIOLOGY & GENETICS
Committee Member

[redacted]
12/11/2017
Martin Doughty, PhD
DEPARTMENT OF ANATOMY, PHYSIOLOGY & GENETICS
Committee Member

[redacted]
12/11/2017
Thomas Flagg, PhD
DEPARTMENT OF ANATOMY, PHYSIOLOGY & GENETICS
Committee Member

ACKNOWLEDGMENTS

I thank all past and present members of Dr. Juliano's lab namely Dr. Susan Schwerin, Dr. Sylvie Polush, Dr. Joseph Abbah, Ms. Mitali Chatterjee and Mr. Joseph Latoche for teaching me some of the research techniques during my lab rotation.

My expression of gratitude goes to members of other labs: Dr. Aviva Symes for giving me easy access to her lab to run alternative western blots experiments as needed, Dr. Mitchell Kendal and for his advice and encouragement, Dr. Kwame Affram for his advice encouragement and assistance with some experiments in difficult times, Dr. John Wu for giving us his spare sonicator for western blots, Ms. Madelaine Cho-Clark and Dr. Darwin Omar Larco for their assistance in troubleshooting and optimizing my western blots, Dr Clifton Dalgard for allowing us to use his qPCR machine and reagents, Mr. Gauthaman Sukumar for assistance with the qPCR experiments, Dr. Andrew Snow for giving me access to his BCA plate reader, Dr. Jeffrey Stinson and Dr. Swadhinya Arjunaraja for teaching me how to set up and use the plate reader, Dr. Fritz Lischka and Dr. Dennis Madaniel for their assistance with microscopy work.

I am very grateful to all members of my thesis committee: Dr. Aviva Symes for her technical counsel, encouragement in difficult times, patience and guidance to stay on track until the end; Dr. Thomas Flagg, Dr. Regina Armstrong, Dr. Martin Doughty and Dr. Sharon Juliano for their diverse support especially the constructive criticisms that were most needed to stay on track.

To my family members, the Konkomba Youth Association, USA, my Kensington Baptist Church members and many friends who have supported me in diverse ways (morally, spiritually and socially) in times of sickness and festive moments, I say many thanks to you all.

Without forgetting the immense support given to me by the Uniformed Services University of the Health Sciences, the Graduate Education Office, the Henry M. Jackson

Foundation, the Center for the Study of Traumatic Stress, all the hardworking members of the Laboratory Animal Medicine (LAM) who helped us with excellent animal care (especially Maj. Maxwell, Maj. Reiter, Sgt. Aguilla and Sgt Fluid) and my helpful class mates (Maj. Geoffrey Dunckle, Dr. Michael Authement, Ms. Christina Marion and Ms. Michelle Bylicky), I say "thank you all".

Furthermore I wish to thank my home institution, the University of Cape Coast, the School of Medical Sciences and the Department of Physiology for granting me the study leave to pursue my terminal degree.

Finally, my heartfelt gratitude goes to my mentor and thesis advisor Dr. Sharon Juliano for helping me define a clear path to my career. I am very grateful for her mentoring, patience, understanding, and support, which were most needed to bring me this far. Her contribution in mentoring me is not only beneficial for my personal transformation and development but also for the transformation of a people, a nation and the world as a whole.

DEDICATION

I dedicate this thesis to my entire family: Mrs. Gladys Barkei Djankpa (wife), Jethro Wumborja Djankpa (son), Othniel N-Muanbindo Djankpa (son), Shalom Mameel Djankpa (daughter) and my parents Rev. Peter Nighain Djankpa, Mrs. Gladys Alamissi Djankpa, Mr. Jacob Djankpa (brother) and Ms. Agnes Djankpa (sister).

COPYRIGHT STATEMENT

The author hereby certifies that the use of any copyrighted material in the dissertation manuscript entitled: The KCC2 Influence on Neuronal Migration in Ferret Neocortex is appropriately acknowledged and, beyond brief excerpts, is with the permission of the copyright owner.

[Signature] 

Francis Tanam Djankpa

January 18, 2018.

DISCLAIMER

The views presented here are those of the author and are not to be construed as official or reflecting the views of the Uniformed Services University of the Health Sciences, the Department of Defense or the U.S. Government.

ABSTRACT

The KCC2 Influence on Neuronal Migration in Ferret Neocortex

Francis Tanam Djankpa, PhD, 2017

Thesis directed by: Dr. Sharon L. Juliano, Professor of Neuroscience & Molecular Biology, Department of Anatomy, Physiology and Genetics.

KCC2 is a brain specific potassium-chloride cotransporter that affects development of the cerebral cortex, including aspects of neuronal migration and cellular maturation and differentiation. KCC2 also modulates chloride homeostasis by influencing the switch of GABA from depolarizing in young neurons to hyperpolarizing in mature neurons. This switch in polarity is believed to contribute to the guidance cues that modulate termination of neuronal migration. The expression of KCC2 during migration of interneurons correlates with the ability of these cells to respond to GABA as a stop signal, suggesting that KCC2 might act as a switch controlling GABA from acting in a motogenic capacity to becoming a stop signal in migrating neurons. Therefore, manipulation of KCC2 expression or its activity early in development can affect various aspects of migrating neurons, including the speed. We earlier developed a model of impaired cortical development by injecting methylazoxymethanol acetate (MAM) into pregnant ferrets during mid-cortical gestation, which briefly interferes with neuronal production, disrupts neuronal migration, and results in increased production of KCC2. We first describe the expression pattern, regional distribution and cellular colocalization of KCC2 with other neuronal markers in ferret neocortex in normal kits and those treated with MAM (Chapter 2). Next we study the effect of KCC2 downregulation on the migration of neurons away from the ganglionic eminence (GE) and into the neocortex at

postnatal day 0 (P0) in ferret organotypic slice cultures (Chapter 3). In Chapter 2 we show a shift in KCC2 expression during development from being strong in the subplate at P0, repositioning into a subtle laminar pattern at P7-P14 and becoming homogeneous at P35. In the immature cortex, the KCC2 immunoreactivity was clearly located in migrating neurons and occurred in the cell membrane and cell processes and extended into the cytoplasm. Whereas in mature neocortex, KCC2 locates predominantly in processes and is difficult to assign to individual neurons. KCC2 colocalizes with several neuronal markers in the developing and mature cerebral cortex of normal ferrets and those treated with MAM, but shows a distinct pattern of expression during maturation and locates in well defined cellular compartments that alter as the animal becomes older. Subcellular localization shows that KCC2 predominantly situates in the membrane fraction at all ages, despite its cytoplasmic presence in young animals. KCC2 also shows increased expression in MAM-treated cortex up to the oldest age we studied, 5 weeks of age. In Chapter 3, we assessed if reducing KCC2 levels restores features of impaired migration that occur after MAM treatment, which increases levels of KCC2. Using western blot, we show that treatment of P0 organotypic slices of neocortex with bisphenol-A (BPA) significantly decreases KCC2 protein levels. MEQ (6-Methoxy-*N*-Ethylquinolinium Iodide) chloride imaging verified that treatment of P0 organotypic slices with the antagonist VU0240551 inhibits KCC2 activity. Analysis of time-lapse video imaging of organotypic slices treated with BPA and VU0240551 show increased average speed and step size of migrating interneurons leaving the ganglionic eminence at P0. These findings confirm that manipulating the actions of KCC2 by reducing protein levels or pharmacologic antagonism can counteract effects of MAM by increasing the speed of migrating neurons. These studies also verify that a toxin derived from the environment can result in persistent negative effects on brain development and on the pathogenesis of neurodevelopmental disorders by changing how neurons migrate to their target sites.

TABLE OF CONTENTS

LIST OF TABLES

LIST OF FIGURES

CHAPTER 1: Introduction

BACKGROUND

Cortical dysplasia results from abnormal brain development in-utero and ranges from local disruption in the migration of cortical interneurons to severe brain malformations. Cortical dysplasia occurs in neurodevelopmental and psychiatric disorders like epilepsy, schizophrenia and autism spectrum disorders (ASD) (14; 23; 71; 72; 101; 109; 116). These disorders affect about 120 million people worldwide and yet have no well-defined treatment because of limitations in our understanding of the etiologies and pathogenic mechanisms of cortical dysplasia. Several factors including environmental toxins, injuries, genetic alterations and infections can affect brain development leading to cortical dysplasia. Extensive research on brain development revealed the mechanisms of neurogenesis, radial and tangential migration and gliogenesis in normal developing brain but the etiology and pathogenic mechanisms responsible for abnormal neuronal migration in cortical dysplasia still remain elusive (14). During corticogenesis, many proteins regulate the migration of GABAergic interneurons from the GE to their destination in the cortex (54; 77; 83; 110). Dysregulation of any of these proteins can result in cortical dysplasia. The NKCC1 and the KCC2 are chloride transporters, which mediate the activity of GABAergic networks by regulating the intracellular chloride concentration. A developmental regulation of NKCC1 and KCC2 expression changes GABAergic network activity from depolarizing (excitatory) in immature neurons to hyperpolarizing (inhibitory) in mature neurons (77). During late embryonic and early postnatal life, the increased expression of the chloride importer (NKCC1) over the chloride exporter (KCC2) in immature neurons maintains a high intracellular Cl^- concentration, which makes GABAergic networks depolarizing (35). On maturation, KCC2 expression increases whereas NKCC1 expression decreases to maintain a low intracellular Cl^- concentration making GABA induced currents

hyperpolarizing. This functional switch is one of the guidance cues important in regulating the migration of interneurons to their appropriate destination in the cortex (24). Our study seeks to investigate the effect of environmental toxins such methylazoxymethanol (MAM) acetate and bisphenol A (BPA) on the expression of KCC2 (thereby altering the functional balance between NKCC1 and KCC2) and its implication on features of migrating interneurons leading to cortical dysplasia in ferrets.

Rodents like mice and rats are lissencephalic and not only lack the neural progenitors responsible for the formation of sulci and gyri but also are missing important mechanisms involved in the migration of these progenitors. We propose the use of ferrets to study the etiology and mechanisms of abnormal neuronal migration in cortical dysplasia for several reasons. Ferrets are the smallest known carnivorous mammals with a gyrencephalic brain similar to that of humans in many ways. The medial and caudal ganglionic eminences remain the main sources of cortical interneurons in rodents whereas in ferrets cortical interneurons originate from the lateral ganglionic eminence in addition to the medial and caudal ganglionic eminences (48; 97; 127). The subventricular zone of ferret neocortex unlike mice and rats is layered into an outer subventricular zone (OSVZ) and an inner subventricular zone (ISVZ), which are features unique to gyrencephalic brains (40). Fietz and colleagues also reported that the OSVZ progenitors in ferret neocortex are epithelial-like and expand by integrin signaling similar to humans (40). The outer radial glial (oRG) cells in ferrets undergo multiple rounds of self-renewing and symmetric divisions that expand the oRG population and this is similar to what happens in humans (49). In addition, cortical development in ferrets continues postnatally up to 2 weeks and this provides opportunity to study both prenatal and postnatal developmental processes (62; 92). Six to twelve (6-12) ferret kits are usually born from one pregnant mother. This large number of ferret kits relative to other higher gyrencephalic mammals enables examination and manipulation of various experimental conditions giving sufficient sample size. Obviously, studying the mechanisms of

abnormal neuronal migration in a gyrencephalic brain as we propose in this study has a greater potential of translating to humans as compared to rodents.

We developed a ferret model of cortical dysplasia by intraperitoneal (IP) injection of methylaxozymethanol acetate (MAM) to pregnant ferret on embryonic day 33 (E33) with the aim of studying the mechanisms of abnormal neuronal migration induced by MAM in the neocortex of ferret kits. MAM is an alkylating and antimitotic agent naturally occurring in cycad seeds, which are consumed in some parts of the world (39). MAM has mutagenic, teratogenic and carcinogenic properties when ingested in larger quantities (39). *In vivo*, MAM is rapidly converted to methyldiazonium, which damages DNA by methylating the O6 or N7 positions of guanine residues (39). Actively dividing neuroepithelial cells in the S-phase of the cell cycle are affected whereas postmitotic neurons and neuroblasts in the G0 phase are spared (27; 64). A single dose of MAM (14mg/kg body weight) administered to E33 pregnant ferrets disrupts the proliferation of specific neuronal progenitors in-utero in neonates causing cortical dysplasia in layer IV. MAM ablates a subpopulation of proliferating interneurons causing alterations in their migration pattern. The consequences of altered interneuron migration can be quite drastic for cortical circuit assembly. Improper distribution of interneurons can result in cell death in areas of higher densities and epileptic activities in areas of lower densities (31; 44). In addition, several neurodevelopmental pathologies such as autism spectrum disorders and schizophrenia have been associated with alterations in interneuron number, placement, and/or maturation (14; 23; 71; 72; 101; 109; 116). In this context, our model of cortical dysplasia share common pathogenic features with schizophrenia and autism spectrum disorders and promises to be useful in increasing our current understanding of the pathogenesis of these diseases.

So far, our findings indicate that MAM treatment reduces the migration speed and changes the exploratory behavior of GABAergic interneurons leaving the GE. MAM also increased total DNA methylation. We found consistent alterations in the GABAergic

system in MAM treated ferrets: upregulation and increased activity of $GABA_A$ receptor subtypes (1; 2) abnormal distribution of subsets of GABAergic interneurons (61; 97) and upregulation of KCC2 protein levels (2).

Testing the causality between KCC2 upregulation by MAM and the observed alteration in features of migrating interneurons, we also treated organotypic slices from P0 normal ferret kits with BPA an industrial toxins shown to downregulate KCC2. BPA is an estrogenic chemical used in making polycarbonate and epoxy resins lining food and beverage cans and bottles. It belongs to the bisphenol family of compounds comprising but not limited to bisphenol B (BPB), bisphenol C (BPC), bisphenol E (BPE), bisphenol F (BPF) and bisphenol S (BPS). There is emerging evidence that BPA is a potential gene toxicant during embryonic development and exposure to it has diverse adverse effects on human and animal health (25; 50; 59; 121). Recently, Yeo and others (132) showed that exposure to BPA affects the developing brain by downregulating KCC2. Our findings show that BPA treatment increases KCC2 protein expression as well as the speed and step size of migrating neurons leaving the GE. Increased speed and step size of migrating neurons obviously lead to misplacement of neurons (cortical dysplasia).

OVERVIEW OF NEURONAL MIGRATION DURING CORTICOGENESIS

Neuronal migration refers to the step-by-step locomotion of young neurons from their site of origin to their destination. This process is precisely regulated by myriads of guidance cues comprised of intrinsic and extrinsic factors to ensure that neurons end up at a specific location and position for proper function of the brain. The guidance cues have a specific time and space distribution and act precisely to ensure migrating neurons find their path and navigate safely to their destination (37; 76; 117). Based on the site of origin, trajectory and neuronal fate, two types of migration define corticogenesis: radial and tangential migrations (Figure 1) (76; 79-81; 83; 119). Tangential migration describes the trajectory of neurons originating from the subpallial telecephalon (lateral, medial and caudal ganglionic eminences) that course to the ventricular zone through several streams

and give rise to GABAergic neurons (interneurons) involved in the formation of local circuits (76; 80). Birth dating, morphological, and distribution studies show that GABAergic neurons coursing through different streams (the marginal zone, subplate, and lower intermediate zone) constitute different populations of tangentially migrating neurons (6; 80). Radial migration on the other hand refers to the movement of neurons from the ventricular zone of the pallium along radial glial cells to give rise to glutamatergic (projection) neurons in the cortex (83; 105). The path of tangentially migrating neurons is parallel to the ventricular surface and orthogonal to the radial glial palisade whereas that of radially migrating cells is perpendicular to the ventricular surface along side the radial glial fibers (83). Migrating neurons can, however, alternate from radial to tangential movement and vice versa as needed indicating some similarities in the motogenic properties in both types of movement (82; 83). Upon reaching the neocortex, migrating neurons are guided by a combination of motogenic and chemoattractive factors along radial glial cells to form cortical layers in an inside out fashion such that neurons born earlier form deeper layers and those born later migrate past deep layers to form superficial layers (53; 81; 83; 103).

During the formation of the neocortex (Figure 2), the early neurons form a transient structure, the preplate, consisting of the marginal zone (MZ), which contains Cajal-Retzius cells and the subplate, composed of early arriving larger cells (83). Cajal Retzius cells are born in the pallium and migrate tangentially to the preplate (20; 114; 133). They secrete reelin, a guidance molecule. Additional cells migrating from the ventricular zone form the cortical plate (CP) by intercalating and splitting the preplate into the MZ (which eventually becomes cortical layer I) and the subplate. The subplate serves as a waiting compartment for migrating cells destined for the CP and also for growing cortical afferents forming the early cortical synapses (15; 69). The development of the neocortex progresses with new waves of neurons that occupy progressively more superficial positions within the CP (53; 81). On the other hand, GABAergic neurons

arrive in the neocortex through several streams and disperse tangentially through the marginal zone, subplate, and the intermediate zone and switch to a radial migration to reach their final position in the cortex (7; 95; 98; 115).

MECHANISMS AND FACTORS INFLUENCING NEURONAL MIGRATION IN THE CORTEX

Neuronal migration occurs through a rearrangement of the cytoskeletal components in response to extracellular cues mediated by several intracellular signaling pathways (10). Neuronal locomotion consists of three (3) main steps: extension of leading process, translocation of the nucleus into the leading process and nucleokinesis resulting into a saltatory movement of the neuron (10). During locomotion, neurons give out a leading process having a growth cone at the tip that serves as the main sensor detecting and responding to all guidance cues keeping neurons on the right path (104; 130). Some of the guidance cues include reelin (secreted by Cajal-Retzius) and together with semaphorins and other factors guide the migration of pyramidal neurons through a receptor tyrosikne kinase cascade of reactions (57; 83). Neuregulin and many integrins also guide migrating neurons along radial glial cells in the formation of cortical layers (4; 8; 41). A summary of several intracellular mechanisms and intricate molecular networks involved in neuronal migration is shown in Figure 3 (10). Despite the complexity of these intricate signaling pathways and cascades, they all ultimately end up activating the cytoskeleton, especially actin and microtubules to drive neuronal locomotion (10).

Genetic manipulation studies (mutation and deletion) reveal numerous essential and indispensable genes in the development and formation of the cortex. Lissencephaly 1 (LIS1) and doublecortin (DCX) are microtubule associated proteins that function in nucleokinesis and guide the leading process of migrating neurons (83). Mutation in the *LIS1* gene causes a severe form of cortical dysplasia known as lissencephaly or "smooth brain" where affected individuals lack brain gyrification. In the DCX deficient animals,

migrating interneurons branch more than normal and the branches are unstable indicating some form of disorientation leading to cortical dysplasia (66; 89).

WHAT IS KCC2?

Although the mechanisms stimulating neuronal motility and guiding migrating neurons are beginning to be understood, the extracellular cues and signaling pathways determining the speed and termination of migration are slower to emerge. Recently, Bortone and Polleux (2009) (24) amplified the motogenic and stop signal mechanisms during neuronal migration in the cortex implicating the K^+/Cl^- exchanger (KCC2) (24).

KCC2 is one of nine (9) cation chloride cotransporters (CCCs). It is encoded by the Solute Carrier Family 12 Member 5 (*SLC12A5*) gene and shares high homology with KCC1, KCC3, and KCC4 (85). Based on hydropathy analysis of the KCC2 protein, however, KCC2 is described as a putative model including 12 transmembrane domains and intracellular N and C termini (5; 85; 94). KCC2 exist in two (2) isoforms: a monomer and a dimer (5). The twelve (12) transmembrane domain of KCC2 is homologous to the glutamate-GABA anti-porter structure (PDB: 4DJK) whereas the C-terminus domain displays sequence and structure homology to the prokaryotic cation chloride cotransporter (PDB: 3G4O) (5). Functional studies show that phosphorylation and glycosylation are essential for the functional integrity of KCC2 and interference of the C-terminus leads to loss of function (5).

KCC2 is a brain specific K^+/Cl^- exchanger, which controls the reversal potential of chloride (Cl^-) ions and therefore determines the developmental switch of GABA from depolarizing, in young neurons, to hyperpolarizing in mature neurons (17; 19; 35; 65; 87). KCC2 functions together with another ion channel protein, NKCC1 ($Na^+/K^+/Cl^-$ transporter), which decreases during brain maturation, while KCC2 increases (35). KCC2 exports Cl^-, while NKCC1 imports Cl^-, resulting in neuronal excitability change and the resulting alteration of GABAergic function during development (Figure 4).

The existing functional models depict KCC2 as a chloride exporter that regulates the activity of GABA (17; 19; 35). In young neurons, the activity of NKCC1 accumulates chloride ions inside the cell such that binding of GABA to its receptor leads to efflux of chloride ions causing depolarization. In mature neurons, the chloride exporting function of KCC2 favors accumulation of Chloride ions outside the cell. When GABA binds to its receptor on the cell surface, it triggers series of signaling cascades that enable influx of chloride ions leading to hyperpolarization. Therefore any alteration in the expression and/or activity of NKCC1 and KCC2 affecting their functional balance (as is the case in this study) will alter GABA signaling and polarity switch and consequently neuronal migration.

KCC2 expression and distribution

The *SLC12A5* gene expresses KCC2 using a complex mechanism. In mice, the KCC2 gene leads to transcription of 2 isoforms, Kcc2a and Kcc2b, with isoform b contributing to about 90% expression in mature animals (131). Screening of the KCC2 gene in mouse shows that a 1.4kb segment of the promoter region is indispensable for the full expression of KCC2 protein. In vitro studies revel that binding of EGR4 to one of the active sites of the 1.4kb segment drives KCC2 upregulation (118).

Many factors influence the expression of KCC2, specifically neuronal activity and the depolarizing action of $GABA_AR$ (46); calcium influx through nicotinic acetylcholine receptor (74); repressor element-1, brain derived neurotrophic factor (BDNF), early growth response-protein 1, and the repressor element-1 silencing transcription factor (78; 131); early growth response protein 4 (EGR4) (118); methyl-CpG-binding protein2 (132); insulin-like growth factor, and cystic fibrosis transmembrane conductance regulator (126).

The repressor element silencing transcription factor (REST-1) plays a dual role in both transcription activation and repression of the KCC gene. REST varies in composition depending on the target gene, cellular activity or state of stimulation and

drives the expression of KCC2 as needed both in plasticity and prenatally (38; 131). Regulation of KCC2 by REST involves a shared corepressor complex that depends on the DNA folding of the KCC2 gene such that in developing neurons the DNA folding favors a stronger activity of the REST leading to KCC2 gene repression and the reverse occurs in mature neurons leading to derepression of the KCC2 gene and consequent KCC2 upregulation. In addition, BDNF is known to accelerate the developmental chloride shift through upregulation of KCC2 gene and mediated by RE-1. The action of BDNF is postulated to occur through the Tropomyosin Receptor Kinase B (TrkB) signaling involving MEK, TRK and possibly the adaptor protein Shc pathway leading to activation of EGR4 and other downstream players which ultimately leads to inhibition of the REST complex and activation of KCC2 expression (78; 107; 108; 131).

Although KCC2 is recognized as an ion channel protein associated with neurons, little is known about its overall distribution in developing or mature cortex and its localization with excitatory and/or inhibitory neurons. In Chapter 2, we assess the expression pattern of KCC2, its cellular localization as well as its colocalization with identified neurons in the cerebral cortex of ferret during development.

The role of KCC2 in neuronal migration

During neuronal migration in corticogenesis, KCC2 regulates actin dynamics and the formation of dendritic spines (3; 9; 24; 75; 126). KCC2 induces responsiveness to GABA as a stop signal because KCC2 expression acts as a switch to induce a voltage-sensitive, calcium-mediated reduction of interneuron motility (24). KCC2 overexpression and increase in its activity correlates with reduced speed of migrating neurons (3; 24). Therefore, manipulation of KCC2 expression and/or activity during development can have deleterious effects on features of migrating neurons. Abbah and Juliano (2014) (3) found that inducing the toxin methylazoxymethanol acetate (MAM) during gestation (E33) in the ferret, upregulates KCC2, which correlates with reduced speed and altered features of migrating neurons leaving the GE in ferret neocortex. In Chapter 3, we assess

the effect of in-vitro KCC2 manipulation (downregulation and inhibition of activity) on features of neurons migrating from the GE into the neocortex during corticogenesis in ferrets.

CONCLUSION

Although numerous factors are involved in the migration of neurons from subcortical to neocortical regions, the changes in neuronal polarity and role of specific ion channel proteins in regulating this process are not well studied. In this work, we specifically investigate the role of KCC2, which prominently influences the stop and go of interneuron migration into the neocortex. We show in Chapter 2 that KCC2 is predominantly expressed in the subplate at P0 and P7 in ferret neocortex and evenly dispersed across the entire cortical thickness at P14 and P35 and that KCC2 colocalizes with calretinin expressing neurons at P0, MAP2 expressing neurons at P0 and P35 and parvalbumin expressing neurons at P35 in ferret cortex. We also show in Chapter 3 that downregulation or inhibition of KCC2 activity increases the speed and step size of migrating neurons compared to control. Our findings show that KCC2 and other molecules involved in its expression and regulation of function are candidate genes to target in understanding the pathogenesis of neurodevelopmental disorders involving cortical dysplasia.

These findings indicate that dysregulation of GABAergic network activity and KCC2 upregulation play a role in abnormal neuronal migration in our model of cortical dysplasia. Therefore, determining the factors and mechanisms that alter KCC2 expression in migrating cortical interneurons in our MAM model would greatly improve the current understanding of the mechanisms underlying abnormal neuronal migration in the cortex. Our ferret model of cortical dysplasia not only provides the opportunity to study the mechanisms of abnormal neuronal migration in a gyrencephalic cortex but also reveals how exposure to a short acting environmental toxin can lead to abnormal brain development. Put together, this study will provide insight into the function of KCC2 in

migration of interneurons in the neocortex of ferrets. It will also elucidate the factors and molecular mechanisms underlying KCC2 upregulation in cortical dysplasia thereby revealing potential therapeutic target for epilepsy, schizophrenia, autism spectrum disorders and other related disorders. The role of exposure to environmental toxins such as MAM and BPA in the pathogenesis of cortical dysplasia will also be revealed.

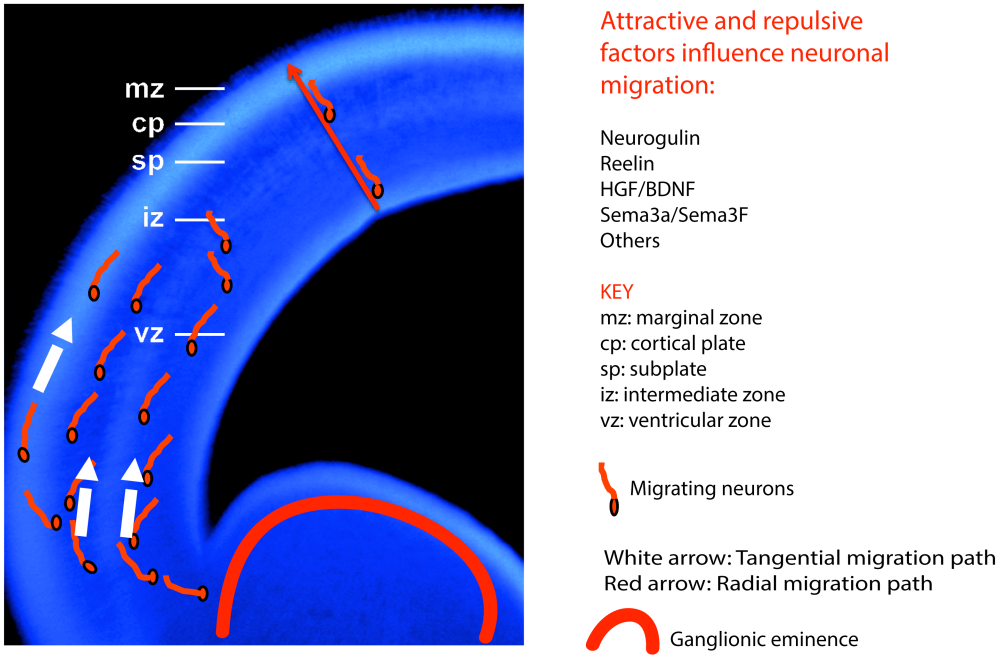

Figure 1: Radial and tangential migration in ferret neocortex sketched after Marin et al, 2010 (83)

The schema shows a coronal slice of the telencephalon at P0 in ferret neocortex, in which the main cortical migrations and their guidance cues are indicated. Interneurons born in the ganglionic eminence (GE) migrate tangentially through the subpallium to reach the cortex along a path indicated by the white arrows. Some of these interneurons enter the striatum (striatal interneurons), whereas others continue toward the cortex (cortical interneurons), sorting out through a mechanism that involves Sema3A and Sema3F. Cortical interneurons advance toward the cortex following a corridor of lateral ganglionic eminence (LGE)-derived cells that express CRD-Nrg1 but not semaphorins. Interneurons are guided toward the cortex by a combination of motogenic (HGF/BDNF) and chemoattractive factors (Ig-Nrg1). Once in the cortex, chemokine signaling (Cxcl12) restricts the migration of interneurons through two streams, the marginal zone (MZ) and the subventricular zone (SVZ). Cajal-Retzius cells also use Cxcl12 to disperse through the MZ in opposite direction to interneurons. Cajal-Retzius cells produce Reelin, which along with other factors such as semaphorins, guide the migration of projection neurons radially along radial glial cells in a path depicted by the red arrow.

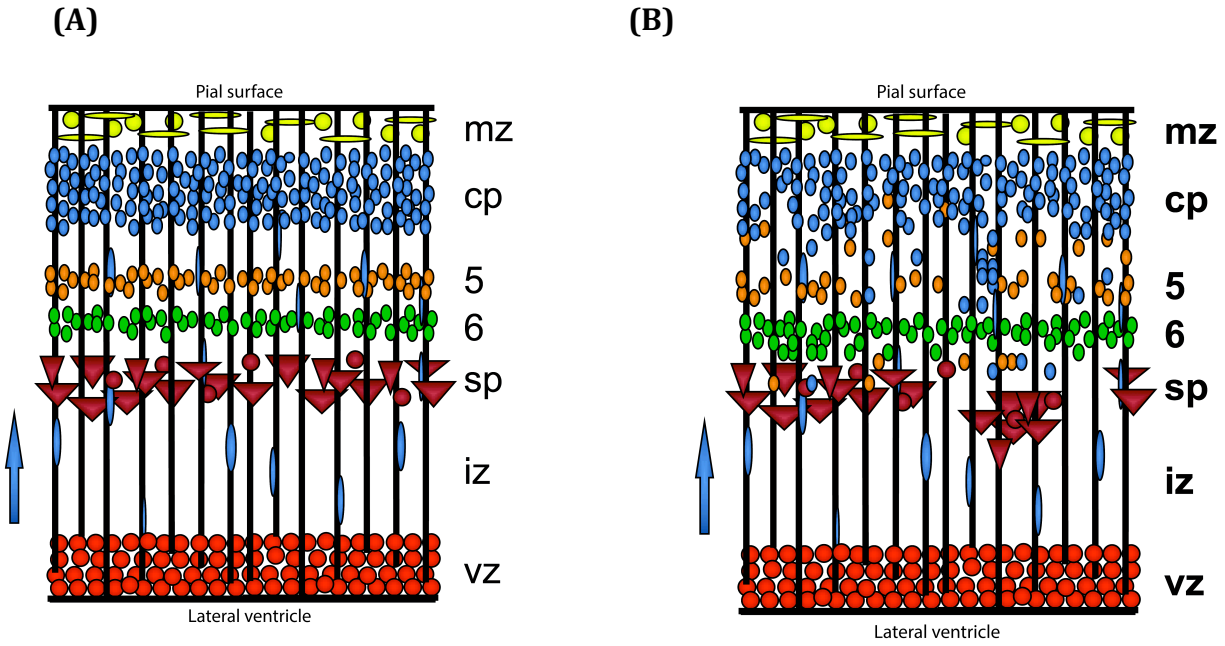

Figure 2: Radial Organization of the Cerebral Cortex Sketched after Ayala et al, 2007 (10).

(A): Projection neurons are born from radial glial cells in the ventricular zone and migrate radially along radial glial fibers toward the pial surface. During each cell cycle, the progenitor cells undergo a distinctive pattern of oscillation, termed interkinetic nuclear migration. Cells undergo S phase at the basal surface of the ventricular zone and mitosis (M) at the apical surface. The first cohort of neurons that migrate out of the ventricular zone constitutes the preplate. The subsequent wave of neuronal migration splits the preplate into two layers: the more superficial marginal zone, which con- sists of the Cajal-Retzius cells; and the deeper subplate. The subplate serves as a waiting compartment for migrating cells destined for the CP and also for growing cortical afferents forming the early cortical synapses. The development of the neocortex progresses with new waves of neurons that occupy progressively more superficial positions within the CP in an inside-out fashion such that newly arriving neurons migrate pass deeper layers to form more superficial layers. Projection neurons may use any of two distinct modes of radial migration, somal translocation, or locomotion, to arrive at their final position in the cortex.

(B): Cortical dysplasia resulting from abnormal neuronal migration due to disruption of any kind affecting any of the factors influencing neuronal migration.

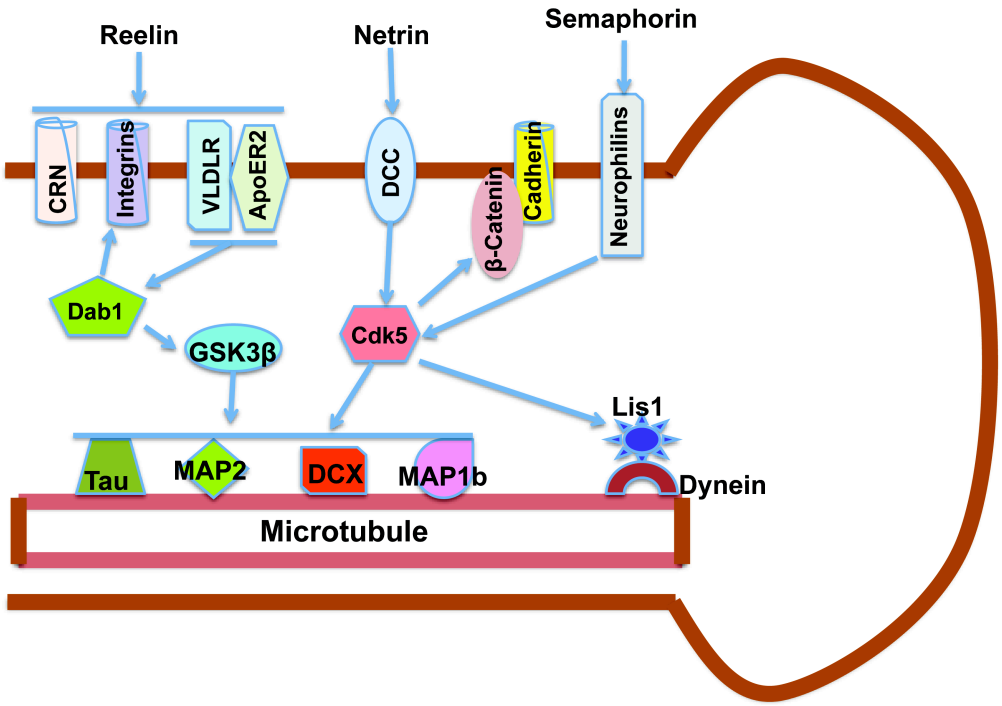

Figure 3: Molecular Networks Regulating Neuronal Migration Sketched after Ayala et al, 2007 (10).

In order for the newborn neurons to arrive at their correct position, extracellular guidance cues, growth, and neurotrophic factors, and cell adhesion complexes, among others, must trigger a wide range of intracellular signaling cascades and, ultimately, end in the coordinated regulation of cytoskeletal dynamics. Some of these pathways, such as Reelin signaling, are very extensively characterized, where others are just beginning to be elucidated. Black arrows indicate direct interactions between proteins. Gray arrows indicate downstream activation of a pathway without evidence of a direct interaction.

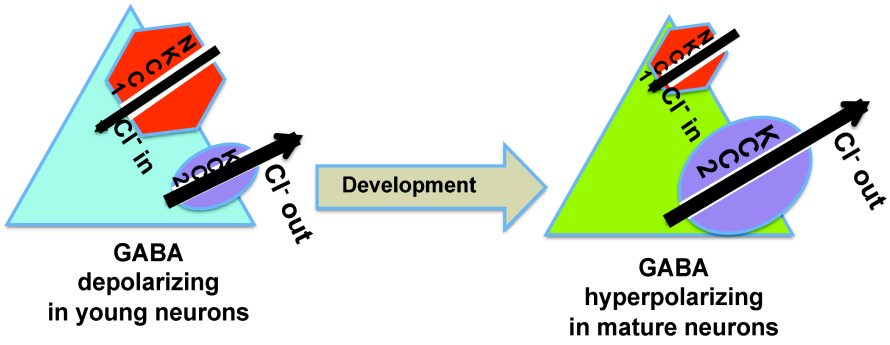

Figure 4: GABA Functional Switch Sketched after Ben-Ari et al, 2012 (19).

The GABA shift of actions is determined in part by a sequential development of two major chloride cotransporters, NKCC1 and KCC2.The former, which imports chloride, but not the latter, which exports it, is present in utero already. In more adult neurons, KCC2 fully operates, whereas NKCC1 is less active, leading to a higher accumulation of chloride in immature neurons causing depolarization. As the neurons mature, KCC2 expression increases over NKCC1 leading to a higher chloride concentration outside neurons causing hyperpolarization.

CHAPTER 2: Distribution and Cellular Localization of KCC2 in Ferret Neocortex

Francis T. Djankpa, Oluwole B. Akinola, Sharon L. Juliano

Abstract

KCC2 (a brain specific potassium-chloride cotransporter) affects development of the cerebral cortex including aspects of neuronal migration and cellular maturation and differentiation. KCC2 also modulates chloride homeostasis by influencing the switch of GABA from depolarizing in young neurons to hyperpolarizing in mature neurons. We describe the expression pattern, regional distribution, and cellular colocalization of KCC2 in ferret cortex in normal kits and those treated with methylazoxymethanol (MAM). We earlier developed a model of impaired cortical development by injecting MAM during mid-cortical gestation, which briefly interferes with neuronal production and additionally results in increased levels of KCC2 at P0. Using immunohistochemistry, we show a shift in KCC2 expression during development, being high in the subplate at P0, repositioning into a subtle laminar pattern in the neocortex at P7-P14 and becoming homogeneous at P35. KCC2 colocalizes with neuronal markers in the developing and mature cerebral cortex of normal ferrets and those treated with MAM, but shows a differential pattern of expression at different ages and locates in distinct cellular compartments during development. Subcellular localization shows that KCC2 predominantly situates in the membrane fraction of neocortical samples. These findings reveal that KCC2 colocalizes differentially with neurons and its expression pattern alters during development.

Key words: development, GABA, interneuron, MAM, neuronal migration

INTRODUCTION

KCC2 plays an important role in development of the cerebral cortex as an ion channel protein causing GABA signaling to switch from excitation to inhibition (17; 18; 65; 128). It works in conjunction with another ion channel protein, NKCC1, which decreases during brain maturation, while KCC2 increases (35). KCC2 exports Cl^-, while NKCC1 imports Cl^-, resulting in neuronal excitability change and alteration of GABAergic function. KCC2 also plays a role in neuronal migration during corticogenesis as well as regulating actin dynamics and the formation of dendritic spines (3; 9; 24; 75; 126).

Our group developed a ferret model of cortical dysplasia by injecting pregnant ferrets with methylazoxymethanol acetate (MAM) on embryonic day 33. MAM is a short acting (8-12 hours) alkylating and antimitotic agent, which selectively disrupts the proliferation of specific neuronal cell populations in S-phase at the time of administration (27; 39; 64). After treatment with MAM in pregnant ferrets during corticogenesis, although the offspring are relatively normal in appearance, a number of features in cortical architecture and function are altered. These include laminar disorganization (97), altered response profiles through neocortical layers (84), specific displacement of GABAergic neurons in mature neocortex (61; 97), and increased levels of $GABA_A$ receptors (1; 3). We also observed that interneurons migrating into the neocortex from the ganglionic eminence specifically altered their speed and pattern of movement after MAM treatment (3). Furthermore, MAM-treated brains have increased levels of $GABA_{A\alpha}$ receptors and KCC2 protein at neonatal ages (3) and $GABA_{A\alpha}$ receptors in older animals (1).

These findings suggest that increased levels of KCC2 after MAM treatment may influence neuronal migration and position in the treated animals. Although KCC2 is recognized as an ion channel protein associated with neurons, little is known about its overall distribution in developing or mature cortex and its localization with excitatory

and/or inhibitory neurons. KCC2 expression has been described in association with neuronal markers including colocalization with the $GABA_A$ receptor β_2/β_3 in rat cerebellum (129), parvalbumin neurons in rat hippocampus (52), and MAP2 in rat striatum (63). The current study assesses the expression pattern of KCC2 in the cerebral cortex of the ferret during development, as well as its colocalization with identified neurons.

The ferret is an important animal to use in this study because ferrets are the smallest mammals with a gyrencephalic brain. Ferrets are altricial and cortical development continues postnatally up to 4-5 weeks or more. This provides the opportunity to study processes that associate with both prenatal and postnatal development (62; 92). Therefore a description of the expression pattern of KCC2 in ferret cortex will provide a useful baseline for understanding the influence of KCC2 in corticogenesis. Given the importance of KCC2 in neuronal migration and function, knowledge of the regional, cellular, and subcellular localization of KCC2 in ferret developing and mature neocortex is essential. Here, we show that the pattern of KCC2 expression evolves over development and that KCC2 is co-localized with multiple neuronal markers. We also report that exposure to an environmental toxin (MAM) upregulates KCC2 expression as the ferret matures.

MATERIALS AND METHODS

Ethics Statement

All experiments in this work were done in accordance with the guidelines approved by the Institutional Animal Care and Use Committee (IACUC) at the Uniformed Services University of the Health Sciences (USUHS).

Animals and MAM Injection

Timed pregnant ferrets (*Mustella putorius furo*) were purchased from Marshall Farms (New Rose, NY). At embryonic day 33 (E33), pregnant ferrets were anesthetized with 5% isofluorane using a mask and given an intraperitoneal (IP) injection of methylazoxymethanol acetate (MAM, MRI Global, Kansas City, MO), at a dose of 14-mg/kg diluted in sterile 0.9% sodium chloride (Hospira, Inc, Lake Forest, IL). MAM-treated pregnant ferrets were allowed to recover and gestation proceeded until 41 days when ferret kits are normally born.

Tissue Processing

Ferret kits (P0, P7, P14, P35-41) were anesthetized with an IP injection of euthasol (50mg/kg) and perfused transcardially with a solution of 4% paraformaldehyde supplemented with 4% sucrose in 0.1 M PBS, pH 7.4 (Santa Cruz Biotechnology, Dallas, TX). After perfusion, each brain was immersed in 4% paraformaldehyde at 4°C, cryoprotected in ascending gradients (10%, 20%, and 30%) of sucrose solutions, then frozen in pre-cooled isopentane and stored at -80°C. Coronal sections (30-50 μm thick) of the somatosensory region were obtained using a cryostat, followed by immunostaining.

Immunohistochemistry and Imaging

Brain sections were hydrated in PBS and placed in blocking buffer (5% normal goat serum, 2% bovine serum albumin, 0.1% Triton X-100) for 1 hour. Sections were then incubated at 4°C overnight with antibodies against KCC2 (Rabbit polyclonal,

Millipore, Billerica, MA, 1:200), parvalbumin (Mouse Monoclonal, Swant, Switzerland, 1:1000), MAP2 (Chicken polyclonal, Abcam, Cambridge, MA, 1:1000), or calretinin (a gift from Dr. David Jacobowitz, USUHS Bethesda, MD, USA). Sections were washed repeatedly in PBS and incubated with the appropriate Alexa-Fluor secondary antibody (Invitrogen, Grand Island, NY), followed by repeated washing and then mounting in Mowiol (Sigma-Aldrich, St Louis, MO). To insure specificity, several sections were run without the primary antibody but with the corresponding secondary antibody. When conducting double label, the primary antibodies were incubated together.

Fluorescent images were captured on a Zeiss Axio Observer.Z1 microscope equipped with an Apotome and Zen 2012 software (Blue edition) version 1.1.2.0 or with a Zeiss 700 confocal microscope equipped with Zen 2012 software (Blue edition). The final images were processed as a maximum intensity projection from 15-20 z-stacks of 2 μm thickness through a given tissue section.

Western blotting

Normal and E33 MAM-treated ferrets were anesthetized and euthanized at P0, P7, P14 and P35. The brains were removed and placed in ice-cold artificial cerebrospinal fluid (ACSF); the somatosensory cortex was dissected and snap-frozen on dry ice. For protein extraction, the frozen somatosensory cortex was thawed on ice and homogenized in ice-cold RIPA lysis buffer supplemented with sodium orthovanadate, protease inhibitors and Phenylmethylsulfonyl Fluoride (PMSF) (Santa Cruz Biotechnology, Dallas, TX). All homogenization used sonication at 4°C, followed by centrifugation at 4°C in an Eppendorf centrifuge 5415C at 20,000 rpm for 30 minutes. The supernatants were collected and protein concentrations determined using the bicinchoninic acid (BCA) protein assay method (Thermo Scientific, Pittsburgh, PA). Adult mouse cortex was used as a positive control.

Membrane proteins and cytoplasmic proteins were extracted using the Mem-PER™ Plus Membrane Protein Extraction Kit (Thermo Scientific, Pittsburgh, PA). Protein samples were denatured by addition of Nupage SDS sample buffer and Nupage sample reducing agent (Invitrogen, Grand Island, NY) and heating at 70°C for 10 minutes or 37°C for 30 minutes for membrane proteins. Electrophoresis of the cation-chloride transporter (KCC2) was accomplished using NUPAGE Novex 3-8% Tris-Acetate gel and NUPAGE Tris-Acetate SDS running buffer supplemented with NUPAGE antioxidant (Invitrogen, Grand Island, NY) and 40μg of protein loaded in each well. Proteins were transferred onto 0.45 μm-pore nitrocellulose membranes using the iBlot dry blotting system (Invitrogen, Grand Island, NY). Membranes were blocked for 1 hour at room temperature in 5% milk blocking buffer dissolved in 1X TBS supplemented with 0.1% Tween-20 (Bio Rad) and incubated with rabbit polyclonal anti-KCC2 (1:500, Millipore, Billerica, MA), at 4°C overnight. Membranes were washed repeatedly in TBS-Tween solution and incubated in goat anti-rabbit secondary antibody conjugated to horseradish peroxidase (Invitrogen, Grand Island, NY, 1:2000) diluted in TBS-Tween, followed by detection using enhanced chemiluminescence reagents (PerkinElmer, Melville, NY). The bands were quantified using ImageJ software (https://imagej.nih.gov/ij/) and the densities compared across the specific ages and also pairwise between MAM and normal tissue using a two-way-ANOVA and the Tukey post-hoc multiple comparison test.

qPCR

Normal and E33 MAM-treated ferrets were anesthetized and euthanized at P0. Brains were removed and placed in ice-cold artificial cerebrospinal fluid (ACSF) and the somatosensory cortex dissected, placed immediately in RNAlater stabilization solution (Ambion, Thermofisher Scientific, Rockville, MD), and stored at 4°C overnight. The next day, total RNA was extracted using the RNeasy mini kit (Qiagen, Valencia, CA).

RNA was reverse transcribed into cDNA using an iScript advanced cDNA synthesis kit (Bio Rad, Hercules, CA) and loaded at 5 ng/well. qPCR was performed using SsoFast-EvaGreen Supermix (Bio Rad, Hercules, CA) with 300 nM of primers in a total volume of 10µl. The following primers with amplicon size of 198 bp were used. Forward: ACCTGTGTGCTCACTTGCAT reverse: ATCAAAGCCATGGCGAGACA, flanking the region 1088-1107 and 1285-1266 of the KCC2 gene respectively. A total amount of 500 ng of RNA was used per reaction. The minimum and maximum ranges of the melting temperature for the primers were 58-60°C. Ribosomal Protein L32 (RPL-32) was used as a housekeeping gene; 4 replicates were used for each sample. Gene expression relative changes were quantified using the ΔΔCt-method relative to the geometric mean of the housekeeping control gene. KCC2 relative expression was compared between control and MAM treated samples using the *student's t-test.*

RESULTS

Developmental pattern of KCC2 expression in the somatosensory cortex

We studied KCC2 immunoreactivity in the neocortex of normal and MAM-treated ferrets aged P0, P7, P14 and P35 - 41. These ages correspond to very early in cortical development, as ferrets are altricial, to an age when cortical layers are relatively mature (Noctor et al 1999; 2001; Poluch and Juliano 2015). At P0, strong immunoreactivity occurs in the subplate, although less obvious in the MAM treated cortex (Figure 5). Many cells are distinct and clearly labeled with immunoreactivity continuing into the processes (insets, Figure 5). This immunoreactivity is preferentially located around the border of each cell and appears to extend into the cytoplasm; which is true for both the normal and MAM treated cortex (Figure 5A', A'', B', B"). As we demonstrated previously (91), the MAM cortex is thinner than normal, also seen at P0 by comparing Figure 5A and B. The subplate, bounded by short yellow lines, is substantially thicker in the normal animal. This can be seen in Figure 5, where the yellow lines defining the subplate in Figure 5B of the MAM-treated animal, extend for ~260 μm, while the normal subplate extends for ~400 μm (Figure 6A). At P7, strong immunoreactivity continues in the subplate, although it is not easily distinguished from the staining in the cortical plate (Figure 6). In a few cells, we observe immunoreactivity within the cell body (indicated with arrows in Figure 6A and B and at higher power in Figure 6A''' and B'''); we generally see less label in, or at the edges of cell bodies, and a stronger reaction surrounding the cells. This phenomenon is seen in the insets shown in Figure 6A', A'' and B', B'' disclosing KCC2 reactivity surrounding cell bodies, revealed by label with bisbenzimide, showing the nuclei in blue. The thickness remains reduced in MAM treated cortex, as can be seen by the yellow lines bounding the cortical plate and the subplate. At P14, a subtle laminar pattern appears in normal cortex, with a slight increase in reactivity shown in layers 4 through 6 (Figure 7A). The laminar pattern is not obvious in the MAM treated cortex, which appears to display stronger immunoreactivity,

although we did not quantify this distribution. The KCC2 label surrounds cells in both the normal and MAM-treated cortex, seen in the higher power images revealing cell nuclei with surrounding KCC2 immunoreactivity (Figure 7A', A'' and B', B''). By P35, the laminar pattern is lost, with extensive KCC2 immunoreactivity surrounding the nuclei revealed by bisbenzimide (Figure 8). Although the immunoreactivity appears to follow a structural pattern, and surrounds nuclei, as seen in the bisbenzimide images (Figure 8A, A', A'' and B, B', B''), it is difficult to determine the precise location of KCC2 in relation to the cells and their processes in this image.

Subcellular localization of KCC2

The pattern of KCC2 expression beginning at P7 appears to surround cells. We also see elongated threads of immunoreactivity that do not show cellular morphology. This suggests that the KCC2 neocortical distribution is not within the cell bodies, but either extracellular or within cellular processes or membranes. Since KCC2 is an ion channel protein, it is likely to be in cell membranes, however the immunoreactive pattern alone does not conclusively show the membrane localization of KCC2 (e.g. Figure 8). To further characterize whether KCC2 is located within the cell membrane, at P0 and P14-P35 we specifically extracted membrane proteins and concomitant cytosolic proteins and conducted western blots. This showed that KCC2 protein is specifically located in the membrane fraction, while the cytosol at these ages shows little evidence of KCC2 (Figure 9 A-B). This is true even at the younger age (P0), where there appears to be substantial immunoreactivity within the soma. Even though the immunohistochemistry indicates that KCC2 is evident in the cell body at P0, this is likely compensated by a greater amount of KCC2 protein found within the processes and membranes in comparison to the amount within the cytosol. To verify that this was also true for animals treated with MAM, we conducted western blots using tissue extracts from MAM treated animals, which also showed the same pattern of increased protein in the cell membrane and very little in the cytosol (Figure 9 C-D). We used Na^+-K^+-ATPase as a positive control for an enzyme

present in membranes and GAPDH as a housekeeping control, since actin might show changes as a cytoskeletal protein.

Colocalization of KCC2 with neuronal markers

Although previous reports suggest that KCC2 colocalizes with neurons, we were interested to determine if KCC2 specifically overlapped with inhibitory cells, since our earlier study demonstrated increased KCC2 associated with impaired migration of inhibitory cells into the neocortex [7,18]. We assessed whether KCC2 colocalized with several neuronal types at P0 and P35-41. At P0, the pattern of reactivity is easier to definitively assign to an individual cell because KCC2 immunoreactivity is less clearly located within a cell as the brain matures. At P0, therefore, we see KCC2 outlining cells and extending into the cytoplasm, whereas at older ages, KCC2 surrounds cells or is in processes, but not observable in the cell body. We first studied the immunoreactivity of KCC2 with a general neuronal marker, MAP2. At P0, KCC2 and MAP2 both extend around the periphery of the soma, while extending slightly into the cytoplasm. Although numerous cells contain both markers, cells also appear that are not labeled with both (Figure 10). The P0 evaluation occurred in the subplate, as this site clearly contains labeled KCC2+ cells. In older animals, at P35, KCC2 immunoreactivity appears as a honeycomb-like pattern, with dense regions surrounding a hollow core, suggesting the KCC2 protein encircles many, if not all, neocortical cells. At P35, KCC2 colocalizes with MAP2+ cells (shown here in layer 5 of somatosensory cortex) as both markers occur in the cell membrane or surround cell bodies (Figure 10B). At this age, although many cells clearly show both markers outlining neurons, we also observe KCC2+ cells that are not labeled with MAP2, suggesting that KCC2 colocalizes with neurons of other phenotypes (Figure 10).

We next evaluated calretinin (CR), a calcium binding protein expressed in cortical interneurons (33; 112). KCC2 clearly colocalizes with CR+ cells at P0 (Figure 11A), also in the subplate. Most cells containing calretinin at P0 appeared surrounded by KCC2

immunoreactivity that extends into the cytoplasm (Figure 11A). When we assessed the pattern of immunoreactivity in an older animal (P41), colocalization was less clear. Many cells were clearly labeled with the antibody against calretinin and KCC2 immunoreactivity surrounded numerous cells, but they were not obviously colocalized (Figure 11B). We noticed, however, that processes extending from the calretinin labeled cells often invaded regions labeled with KCC2 that surrounded presumptive neurons not specifically marked by calretinin (Figure 11B, inset). When assessing the KCC2 distribution, it is obvious that immunoreactivity occurs in many areas that are not calretinin positive suggesting that KCC2 must colocalize with other cell types.

Parvalbumin (PV) is another calcium binding protein associated with a large number of GABAergic cells in the neocortex (33; 112). The PV protein is not strongly expressed at P0, we therefore assessed its colocalization with KCC2 only at P35. When paired with PV label at P35, KCC2 immunoreactivity is studded around many PV+ neurons and also extends into the processes (Figure 12). This pattern of immunoreactivity is different than seen for MAP2+ cells, in that although the colocalization clearly extends into numerous processes in the PV immunoreactive cells, in MAP2+ cells KCC2 reactivity more clearly completely surrounds the soma. The images taken in Figure 12 are from a MAM-treated animal. We did not observe any differences in the colocalization patterns of MAM-treated or normal animals for any of the neuronal markers we assessed.

Quantification of KCC2 mRNA and protein levels after MAM treatment

Although immunoreactivity shows the KCC2 distribution throughout the neocortex, it is difficult to precisely quantify and compare between normal and MAM treated levels using this method, especially since the pattern of immunoreactivity does not lend itself clearly to quantification. To verify our impression that at most ages, the immunohistochemical density of KCC2 expression appeared greater in MAM treated cortex compared to normal, we conducted western blots of tissue taken from the somatosensory cortex at different ages. We previously found that KCC2 protein levels

were increased at birth (P0) in MAM treated animals (3). Figure 13A & B show that KCC2 protein levels are significantly greater at all the ages we assessed (P0, P7, P14, and P35) revealing that the increase we previously observed at birth persists in mature animals.

In addition to quantifying the level of KCC2 protein, it is also important to verify that there is an increase in gene expression. We therefore obtained measurements of mRNA using qPCR. Figure 13C shows that the relative expression of KCC2 mRNA was significantly greater in MAM treated cortex at P0.

DISCUSSION

Summary of findings

During early development, especially at P0 and P7, KCC2 expression is high in the subplate. As the layers of the neocortex develop, we observe a slight laminar pattern at P7 and P14 that relates to the maturity of the cortical layers, but subsequently the laminar pattern is lost at P35. KCC2 also colocalizes with both inhibitory and general neuronal markers. The distribution of KCC2 within a cell seems to alter as the neocortex matures, initially clearly integral to the cell and extending into the cytoplasm, while at older ages only apparent in the cell membrane and processes. We previously found that MAM treatment increased KCC2 expression at P0 (3). Here, we show that MAM treatment increases KCC2 mRNA at P0 as well as protein levels at P0, P7, P14, and P35. Our findings point to prenatal MAM administration as a factor altering the expression level of KCC2 and its distribution within the neocortex, but not altering its cellular compartmentalization.

KCC2 during development

During cortical development, cells containing GABA convert from inducing excitation to inhibition. This process is mediated by changes in chloride ion (Cl-) homeostasis and the balance of the ion channel transporters KCC2 and NKCC1. KCC2 plays a significant role in several important events of corticogenesis including migration, differentiation, maturation, synapse formation, and functional integrity (13; 22; 24; 47; 126). In addition, use of MAM to alter cortical development results in a model of increased KCC2 expression that can be used to further investigate its role in neuronal development. Several studies show that KCC2 levels are low at birth and increase during the postnatal period, with concomitant decreases in NKCC1 (17). In our ferret analysis, we assessed KCC2 distribution and overall levels in the neocortex at times from P0 until P35-41. These developmental dates correspond to about E17 – P11 in the mouse and E20

- P14 in the rat (30). In the ferret, overall levels of KCC2 seem to show more subtle and gradual increases than in the mouse, as we see steady and incremental increases from P0 until P35. The laminar pattern expressed in the mouse is initially greater in the upper layers and becomes homogenous by P40 using in situ hybridization (122). This differs from our observations in the ferret using immunohistochemistry to reveal the KCC2 distribution. We see initial strength in the subplate and lower layers, which undergoes redistribution in a laminar pattern until P35, when the distribution is homogenous. Earlier reports show KCC2 expression in human subplate at week 26 post-conception, corresponding to the type of distribution that we see here (15; 125). Ferrets, and most likely humans, seem to show overall increases in KCC2 that correspond to maturation of cortical layers. Since rodents have a much shorter period of laminar development, the distribution of KCC2 occurs over a collapsed period of time. Thus the distinctions observed in the expression of KCC2 during cortical development most likely reflect differences in the timing and distribution of cells during migration and maturation in each species.

KCC2 colocalization with neuronal markers in ferret cortex

KCC2 clearly localizes with many types of neurons. At early ages, for both a general neuronal marker and together with inhibitory markers, KCC2 appears in the cell membrane and extends slightly into the cytoplasm. As the cortex matures, KCC2 locates more peripherally to the cell and eventually surrounds cells or is studded around the cell membrane. KCC2 is also found in many cell processes, presumptive dendrites, most likely because of its function as a protein of ion channels that regulates the flow of chloride in and out of the cell. Our determination of whether KCC2 is detected in the cell membrane versus the cytosol plainly shows the protein is primarily in the membrane. Its position shifts over time, however, from a thick band around the soma that extends into the cytoplasm, to a much thinner band around a cell. It may be that this change in distribution reflects a change in KCC2 function as the cell matures. KCC2 plays many

roles both during development and as an adult. It is also interesting that the distribution of KCC2 protein within the cell alters as the brain matures. We only see localization of KCC2 protein apparently within the cell body early in development, especially in the subplate. As KCC2 plays a role in migration (24), location of the protein early during development more clearly outlining cells and extending into the cytoplasm may be related to this process. KCC2 can act independently of its ion extruding function and is also involved with differentiation and spine formation (73). These processes may require additional KCC2 protein to be located within the cell body early during development, but not when cells are mature. This may also explain why we clearly show colocalization of a calcium binding protein (i.e. calretinin) with KCC2 at young ages (P0) but not at older ages. Our observation that processes emanating from calretinin positive cells appear to surround calretinin negative cells suggests that the function and relationship between KCC2 and specific neurotransmitters alter as the neocortex matures.

As indicated, KCC2 plays important functions during corticogenesis, including guiding migrating neurons to their targets as well as maintenance of the functional integrity of pyramidal neurons (22; 24). The expression of KCC2 during the migration of interneurons correlates with the ability of these cells to respond to GABA as a stop signal, suggesting that KCC2 might act a switch controlling GABA from acting in a motogenic capacity to becoming a stop signal in migrating neurons (24). As young neurons mature and differentiate to assume their position in the cortex, the KCC2-NKCC1-GABA mediated depolarization by interneurons plays a role in forming the character of dendritic arbors and helps mediate the composition of excitatory synaptic inputs from other pyramidal neurons (26; 123; 124).

We show that KCC2 immunoreactivity occurs in MAP2 expressing cells, which could be both excitatory and inhibitory, and also in calretinin and parvalbumin expressing cells, which are inhibitory. This suggests that KCC2 may occur in (or surround) almost all neurons, or at least many neuronal types. This relates to the finding that KCC2

participates in the general morphologic maturation of neurons and both excitatory and inhibitory synapse formation (73; 124). Overall, the general pattern of distribution suggests that KCC2 is integral to the modulation of neural tone and that changes in the overall level of KCC2 in the brain can have dramatic effects on neuronal function.

MAM treatment increases KCC2 expression in ferret cortex

Prenatal IP administration of a single dose of MAM to pregnant ferrets during mid corticogenesis leads to increased KCC2 expression in ferret kits up to P35. Our earlier findings show that increased KCC2 correlates with abnormal migration of interneurons and altered GABAergic processing in migrating cells leaving the ganglionic eminence as well as the functional properties of mature pyramidal cells (3). We also found increased levels of $GABA_A$ receptors after the same treatment (3). There may be other changes more involved with excitatory cells that we did not investigate. Our observation that a single dose of a toxin (MAM) can alter gene expression and increase protein levels is interesting. Since MAM is a methylating agent, it may be that delivery of this drug results in altered methylation of the KCC2 gene and resultant increased expression of KCC2 protein. In turn, this may result in increased GABA receptors and altered GABAergic processing. Our finding is also important as it demonstrates how small levels of toxins in the environment can affect gene and protein expression resulting in dramatic changes in cortical growth and maturation.

CONCLUSION

Since KCC2 plays an array of important roles in the overall development and function of the cerebral cortex, determining the endogenous and exogenous factors that alter or regulate KCC2 expression will greatly improve our understanding of the mechanisms regulating neuronal migration and the formation of synapses and dendritic arbors. This model therefore represents an important element to study the overall effect of increased KCC2 in an endogenous state. In our future work, we plan to investigate the mechanisms by which MAM increases KCC2 expression.

Conflict of Interest

None declared.

Funding

This research was funded by PHS NS 24014; DOD – USUHS - RO703041

Acknowledgements

We thank Mitali Chatterjee for excellent animal care and assistance with the experiments.

Table 1: Number of normal jills employed for this study and for what purpose the kits were used.

Jills	Number of kits used	Details
F1 Normal	2 P0 kits	1 used for western blot 1 used for Immunohistochemistry
	2 P7 kits	1 used for western blot 1 used for Immunohistochemistry
	2 P14 kits	1 used for western blot 1 used for Immunohistochemistry
	2 P35 kits	1 used for western blot 1 used for Immunohistochemistry
F2 Normal	2 P0 kits	1 used for western blot 1 used for Immunohistochemistry
	2 P7 kit	1 used for western blot 1 used for Immunohistochemistry
	2 P14 kit	1 used for western blot 1 used for Immunohistochemistry
	1 P35 kit	Used for western blot
	1 P41 kit	Used for Immunohistochemistry
F3 Normal	2 P0 kits	1 used for western blot 1 used for Immunohistochemistry
	2 P7 kits	1 used for western blot 1 used for Immunohistochemistry
	1 P14 kit	Used for western blot
	2 P35 kits	1 used for western 1 used for Immunohistochemistry
F4 Normal	1 P14 kit	Used for Immunohistochemistry
	2 P35 kits	1 used for western 1 used for Immunohistochemistry
F5 Normal	1 P0 kit	Used for western blot
	1 P7 kit	Used for western blot
F6 Normal	1 P14 kit	Used for western blot
F7 Normal	1 P35 kit	Used for western blot
F8 Normal	1 P35 kit	Used for western blot
F9 Normal	2 P0 kits	1 used for western blot 1 used for qPCR
F10 Normal	2 P0 kits	1 used for western blot 1 used for qPCR
F11 Normal	2 P0 kits	1 used for western blot 1 used for qPCR
F12 Normal	2 P0 kits	1 used for qPCR 1 used for Immunohistochemistry

Table 2: Number of normal MAM treated jills employed for this study and for what purpose.

Jills	Number of kits used	Details
F1 MAM-Treated	2 P0 kits	1 used for western blot 1 used for Immunohistochemistry
	2 P7 kits	1 used for western blot 1 used for Immunohistochemistry
	2 P14 kits	1 used for western blot 1 used for Immunohistochemistry
F2 MAM-Treated	2 P0 kits	1 used for western blot 1 used for Immunohistochemistry
	2 P7 kits	1 used for western blot 1 used for Immunohistochemistry
	1 P14 kit	Used for western blot
	1 P35 kit	Used for western blot
F3 MAM-Treated	2 P14 kits	1 used for western blot 1 used for Immunohistochemistry
	2 P35 kits	1 used for western blot 1 used for Immunohistochemistry
F4 MAM-Treated	3 P35 kits	1 used for western blot 2 used for Immunohistochemistry
F5 MAM-Treated	2 P0 kits	1 used for western blot 1 used for Immunohistochemistry
	2 P7 kit	1 used for western blot 1 used for Immunohistochemistry
	1 P35 kit	Used for western blot
F6 MAM-Treated	2 P14 kit	1 used for western blot 1 used for Immunohistochemistry
F7 MAM-Treated	2 P35 kit	1 used for western blot 1 used for Immunohistochemistry
F8 MAM-Treated	2 P0 kits	1 used for western blot 1 used for qPCR
F9 MAM-Treated	2 P0 kits	1 used for western blot 1 used for qPCR
F10 MAM-Treated	2 P0 kits	1 used for western blot 1 used for qPCR
F11 MAM-Treated	2 P0 kits	1 used for western blot 1 used for KCC2 qPCR

Table 3: Indicates the total number of kits used at different ages for each type of experiment.

Immunohistochemistry	**Normal**	**MAM**
P0	4	3
P7	3	3
P14	3	3
P35-41	4	5
Western Blot		
P0	7	7
P7	4	3
P14	4	4
P35	6	5
qPCR		
P0	4	4
Total kits	39	37

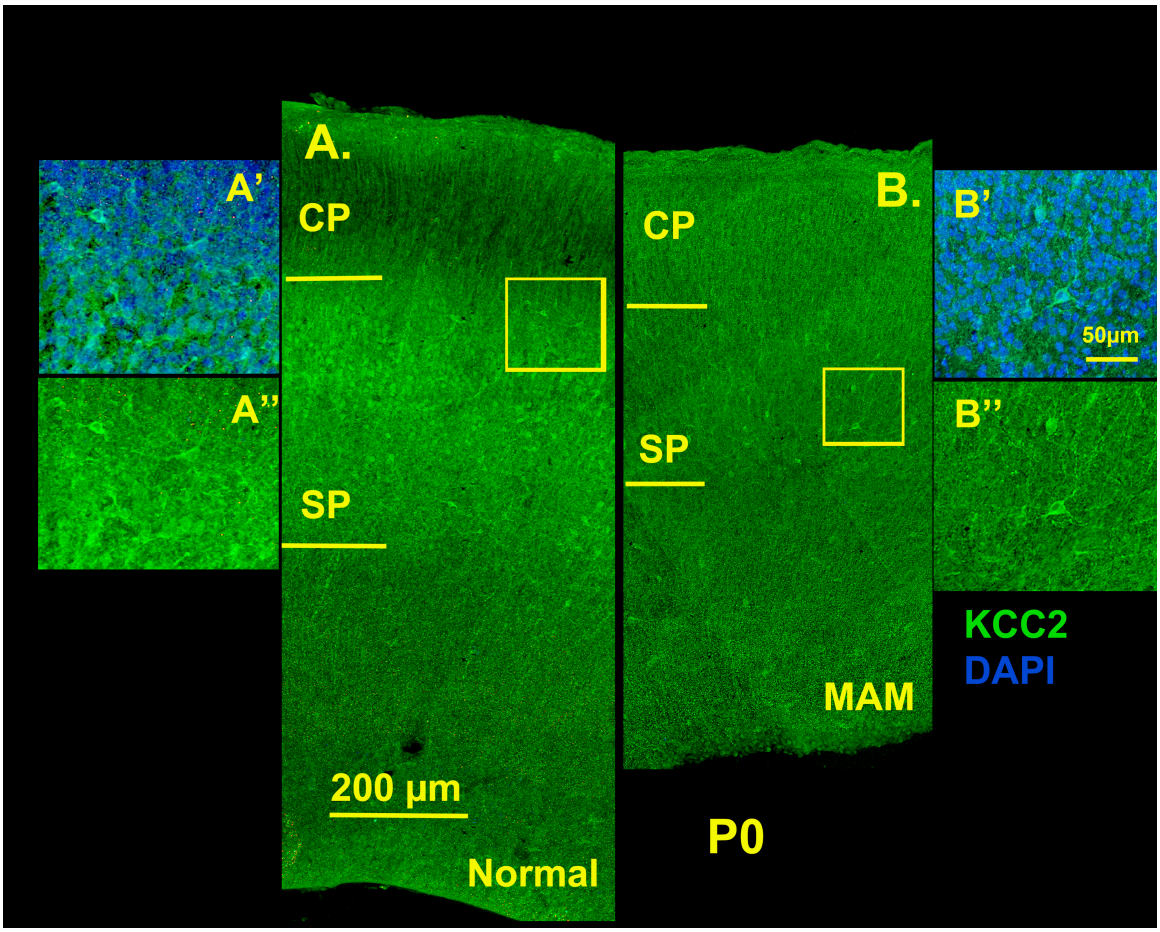

Figure 5. KCC2 Immunoreactivity at P0

At P0, the strongest immunoreactivity occurs in the subplate. Many cells are distinct and clearly labeled with immunoreactivity extending into the processes. The yellow box outlines a region shown at higher power on the outer parts of each figure showing the details of the immunoreactivity in the subplate (A', A'', B', B''). The KCC2 label is preferentially located around the border of each cell and appears to extend into the cytoplasm; this is true for both the normal and MAM treated cortex. The lower inset shows the KCC2 immunoreactivity alone in green, and the upper inset shows the KCC2 label together with bisbenzimide labeling, which reveals nuclei. The MAM-treated neocortex is thinner than normal cortex and the subplate, bounded by the short yellow lines, is substantially thicker in the normal animal. The KCC2 immunoreactivity is green, and the bisbenzimide (labeled Nuclei) is in blue. CP – cortical plate; SP – subplate.

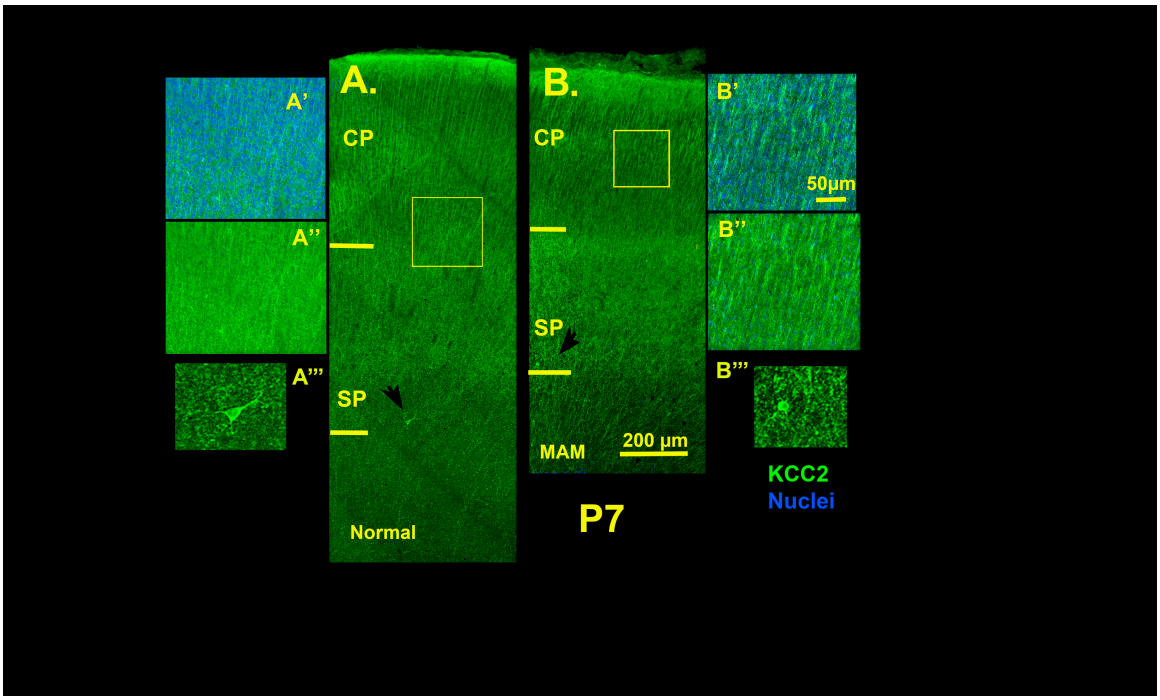

Figure 6. KCC2 Immunoreactivity at P7

At P7, strong immunoreactivity continues in the subplate. We generally see less label in, or at the edges of, cell bodies and a stronger reaction in a pattern surrounding the cells (insets) revealed by bisbenzimide staining (blue). The thickness remains reduced in the MAM treated cortex; the yellow lines border the subplate (SP) and indicate the limit of the cortical plate. A yellow box outlines a region shown in higher power on the outer parts of the figure (A', A'', B', B''). The lower part of the inset shows KCC2 immunoreactivity in green and the upper inset shows KCC2 label in conjunction with bisbenzimide (blue), which reveals nuclei. Black arrows indicate that in a few cells, we observe immunoreactivity within the cell body, similar to that seen at P0 (A''', B''').

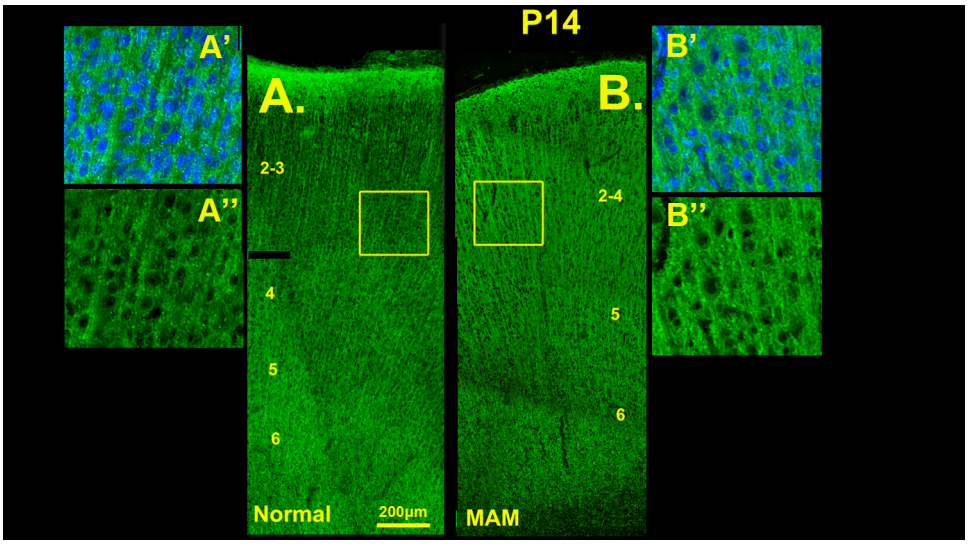

Figure 7: KCC2 Immunoreactivity at P14

At P14, a subtle laminar pattern is evident in the Normal cortex, with increased reactivity in layers 4-6; the black line indicates the border of layer 3 and 4 in normal cortex revealing a slight increase of KCC2 immunoreactive density deep to this level. The laminar pattern is not obvious in the MAM treated cortex, which appears to display stronger immunoreactivity, although we did not quantify this distribution. The regions of cortex bounded by the yellow squares are shown at higher power on the right and left of the image. In the higher power images, the KCC2 label surrounds the cells in both the normal and MAM-treated cortex (A', A'', B', B"), observed as the immunoreactivity for KCC2 (green) surrounds the cell nuclei (blue).

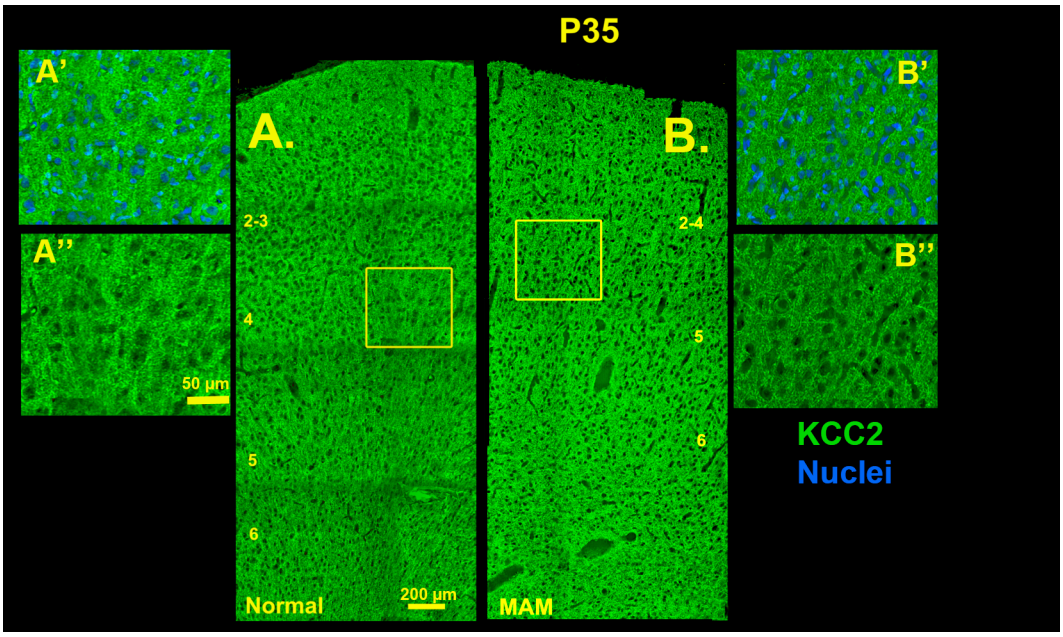

Figure 8: KCC2 Immunoreactivity at P14

At P35, the laminar pattern is lost in both the Normal (A) and MAM (B) treated cortex; the regions inside the yellow boxes are shown at higher power on the right and left of the image (A', A'', B', B''). The extensive green KCC2 immunoreactivity can be seen surrounding the nuclei revealed by bisbenzimide (blue). The approximate locations of cortical layers are indicated with numbers.

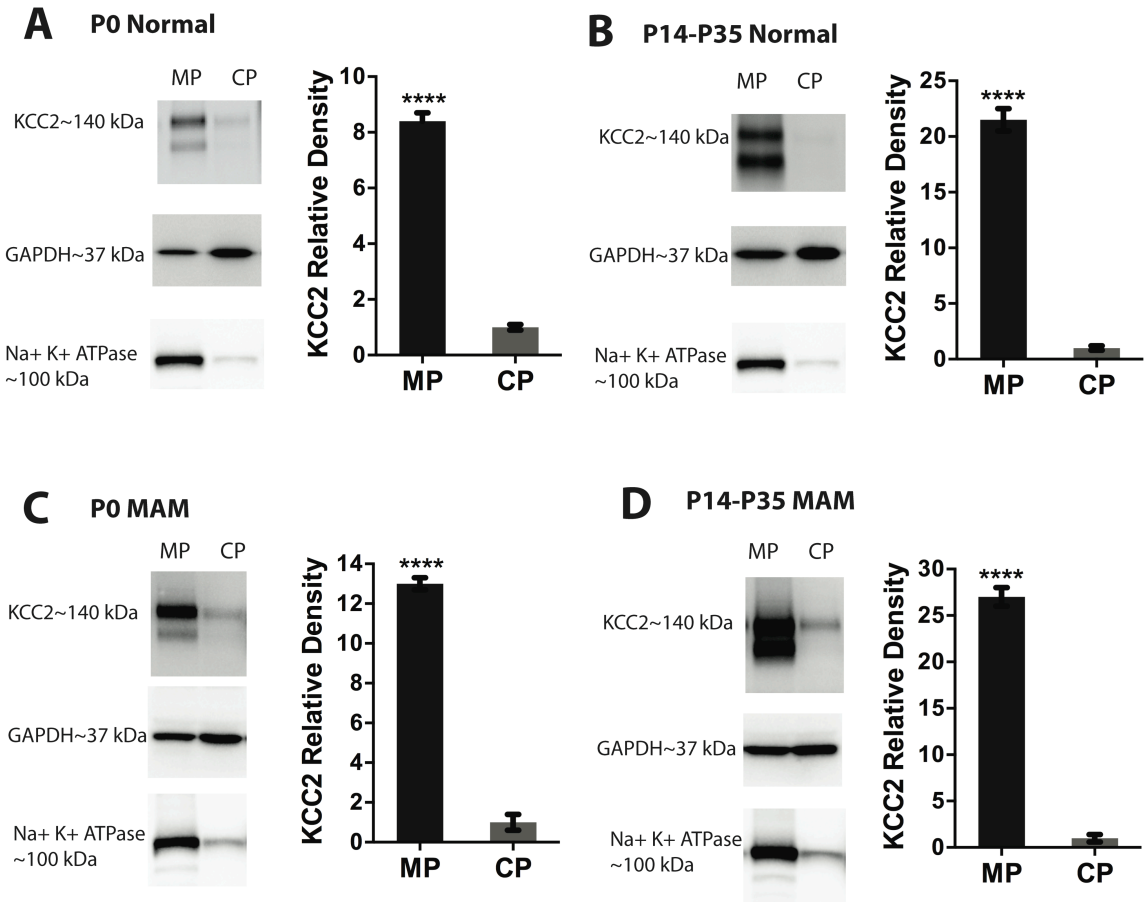

Figure 9: KCC2 in membrane and cytoplasmic proteins.

Western blots of membrane proteins versus cytoplasmic proteins show that KCC2 is located in the cell membrane at P0 and P14-35 in normal (A, B) and MAM-treated tissue (C, D). Samples were taken from the parietal cortex of ferrets, n=3 animals taken from different litters for each group; ****p<0.0001, student's t-test. MP - membrane proteins, CP - cytoplasmic proteins. Na^+-K^+-ATPase used as positive loading control confirming successful separation of membrane fraction from cytoplasmic fraction.

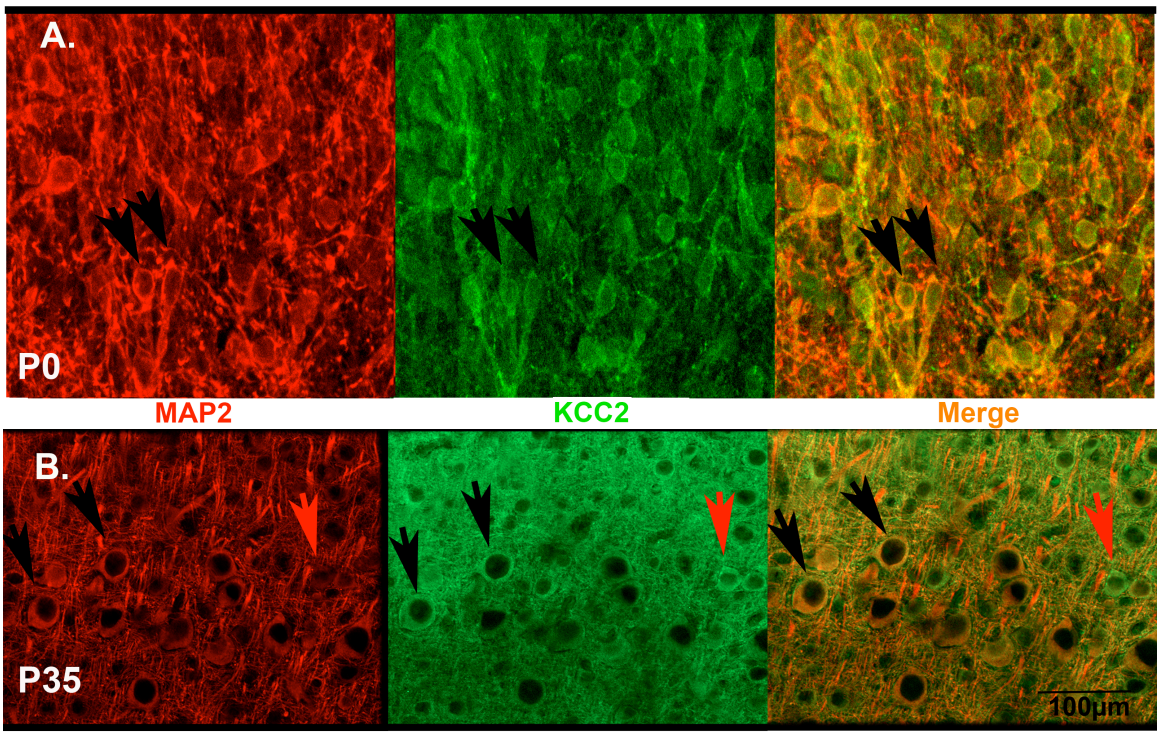

Figure 10: Double label of KCC2 and MAP2 at P0 and P35

(A) At P0 in the subplate, several neurons stained with antibodies against MAP2 (red) possess the morphology of migrating cells. For many cells showing immunoreactivity against KCC2 (green), the label surrounds the presumptive neuron and extends into the cytoplasm. Examples of cells showing apparent double label are indicated with black arrows in each panel. (B) At P35, MAP2 strongly labels many neurons in layer 5 of parietal cortex. Labeled processes are also seen. When combined with KCC2 immunoreactivity, KCC2 surrounds many labeled cells and also extends into the processes. The positions of several cells showing combined KCC2 and MAP2 immunoreactivity are indicated with black arrows. An example of a cell labeled with KCC2 immunoreactivity, but not with MAP2 is indicated with a red arrow (B).

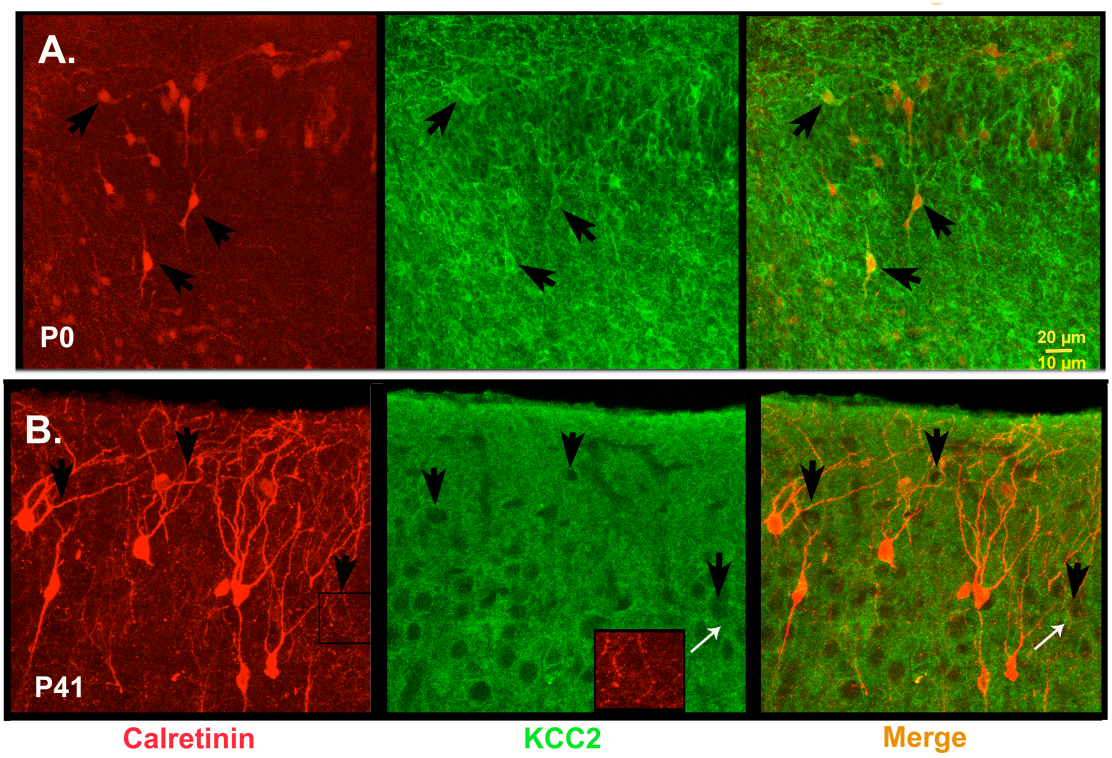

Figure 11: Examples of double label against calretinin and KCC2

(A) At P0, cells labeled with immunoreactivity against calretinin (red) and KCC2 (green) can be seen. The label for KCC2 surrounds many cells and extends into the cytoplasm. Examples of cells that show immunoreactivity for both antibodies are indicated with black arrows. (B) At P41, many cells are immunoreactive for calretinin in the upper layers of parietal cortex (red). Although it is difficult to show colocalization between the two antibody reactions, processes emanating from calretinin positive cells surround regions of KCC2 reactivity that presumably encircle cells immunoreactive for other markers. Examples of these regions are indicated with black arrows. One of the cells encircled with calretinin immunoreactivity is outlined with a box in the bottom left panel. This region is shown at higher power in the adjacent panel (red box) next to the same outlined cell. The white arrows point to the cell outlined by calretinin immunoreactivity. The same cell is also indicated with a black arrow. The scale is 20 µm for the P0 image and 10 µm for the bottom image.

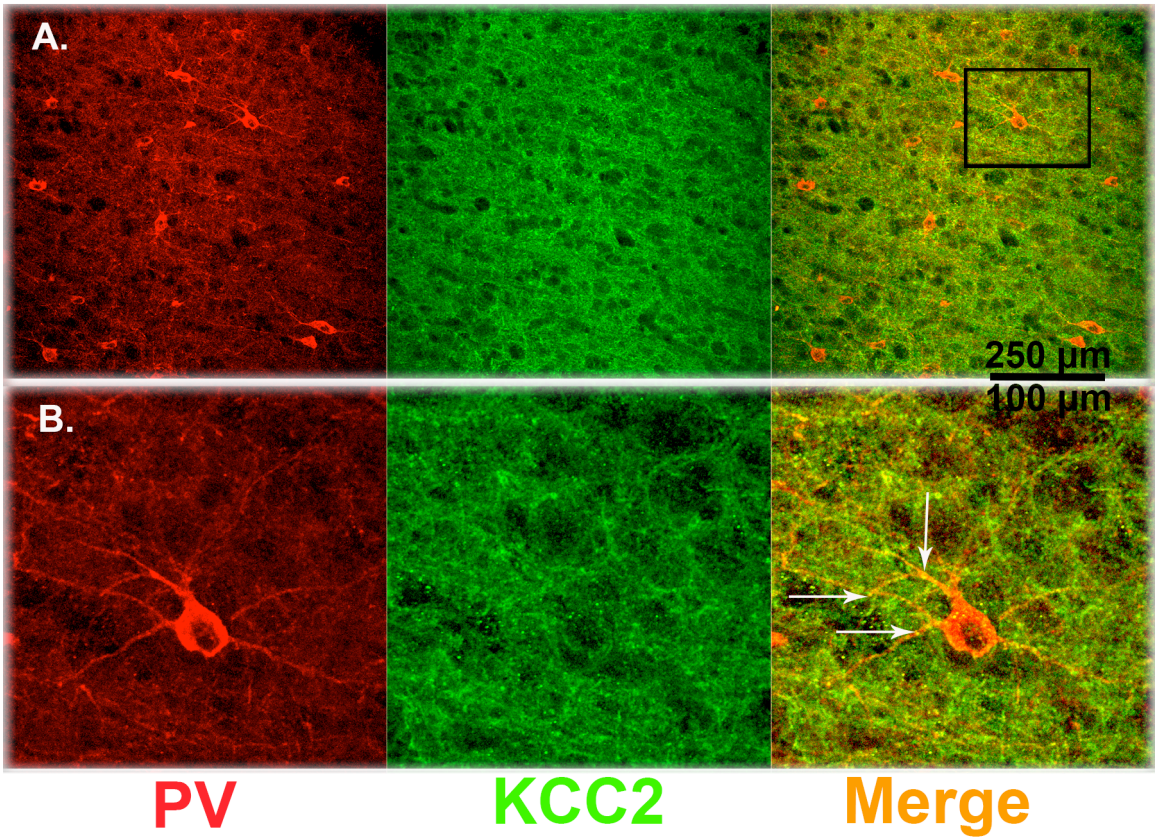

Figure 12: Parvalbumin immunoreactive cells in MAM treated cortex

(A) Shown is an example of low power (top panel) and (B) higher power (bottom panel) views of immunoreactivity against parvalbumin in the lower layers of MAM treated parietal cortex. At low power, multiple cells can be seen immunoreactive for parvalbumin (red) (A); at higher power, KCC2 positive regions can be seen studded along the processes extending from a parvalbumin positive cell. The cell shown at higher power on the bottom is outlined with a black box in the top panel and white arrows point to a few regions of KCC2 immunoreactivity studded along the cell processes. Scale = 250 µm for the upper panel and 100 µm for the lower panel.

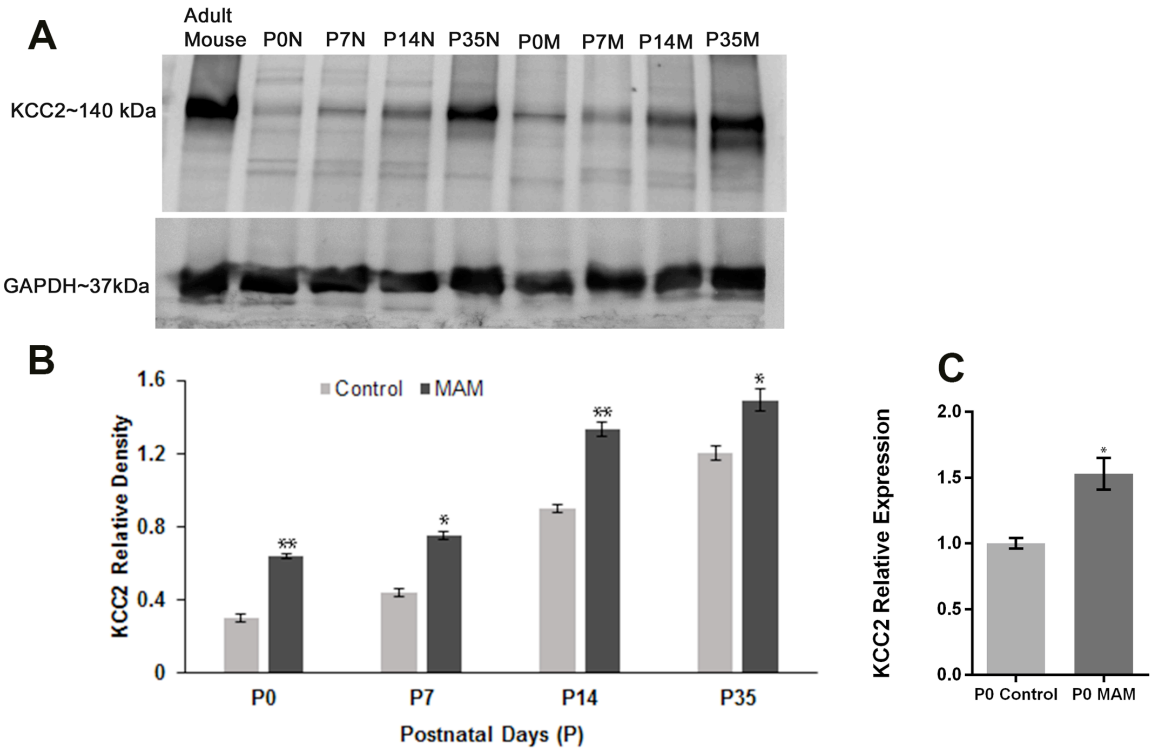

Figure 13: KCC2 Western blot and qPCR

A) Western blots showing levels of KCC2 at P0, P7, P14, and P35 for normal (N) and MAM treated (M) parietal cortex. Adult mouse cortex is shown as a positive control. **B)** The relative density of KCC2 levels compared to the control protein GAPDH, are shown. At each age, KCC2 levels are significantly greater than control levels. 3 animals from different litters were used in each group. We used a Two Way ANOVA $F(3, 16) = 326.8$ $p<0.01$, followed by Tukey's Post-hoc multiple comparison test. * $p < 0.01$; ** $p< 0.001$. **C)** qPCR analysis shows that MAM treatment significantly increases KCC2 mRNA levels in P0 samples * $p = 0.039$, student's t-test, $n = 4$ animals in each group.

CHAPTER 3: KCC2 Manipulation Alters Features of Migrating Interneurons in Ferret Neocortex.

F.T. Djankpa, F. Lischka, M. Chatterjee and S. L. Juliano

Abstract

KCC2 (a K+ - Cl- exchanger) is a brain specific chloride-potassium cotransporter that affects development of the cerebral cortex including aspects of neuronal migration and cellular maturation and differentiation. It modulates chloride homeostasis influencing the switch of GABA from depolarizing in young neurons to hyperpolarizing in mature neurons. This switch in polarity contributes to the guidance cues that modulate termination of neuronal migration. The expression of KCC2 during migration of interneurons correlates with the ability of these cells to respond to GABA as a stop signal, suggesting that KCC2 acts as a switch controlling GABA from functioning in a motogenic capacity to becoming a stop signal in migrating neurons. Manipulation of KCC2 expression or its activity early in development can therefore affect various aspects of migrating neurons including the speed. We describe the effect of KCC2 downregulation and inhibition on features of migrating interneurons leaving the ganglionic eminence (GE) of normal ferret kits and those treated with methylazoxymethanol acetate (MAM), which increases KCC2. (BPA) is following exposure. Treatment of organotypic cultures (from P0 ferret kits) with Bisphenol A (BPA), an environmental toxin that alters gene expression, downregulates KCC2 protein. In organotypic slices treated with the KCC2 antagonist VU0240551, chloride imaging shows inhibition of KCC2 via blockade of chloride flux. Time-lapse video imaging of organotypic cultures treated with either drug that reduces effect of KCC2 shows a significant increase in the average speed and the average step size of migrating neurons leaving the ganglionic eminence at P0 compared to control. Our findings reveal the

harmful effect of environmental toxins on brain development and potential consequences in the pathogenesis of neurodevelopmental disorders.

INTRODUCTION

The process of neuronal migration is precisely regulated by numerous factors that ensure proper positioning and functional integrity of the nervous system. During corticogenesis, interneuron precursors generated mainly in the ganglionic eminence (GE) migrate through tangential streams to the cortical plate and then proceed radially using multiple directional cues to reside in the cortical layers (54; 81; 83; 86; 99; 106). Throughout their trajectories a myriad of extracellular molecules such as slits, netrins, semaphorins, and reelin function as guidance cues for migrating interneurons. Alteration in secretion or expression of these cues misleads the path of the migrating interneurons (54; 77; 83; 111).

Several mechanisms stimulate the motility and guide the migration of cortical interneurons. Activation of AMPA receptors leads to neurite retraction during interneuron migration in the intermediate zone of the neocortex (96; 100). Hepatocyte growth factor functions as a motogen to migrating interneurons in the telecephalon and neuregulin acts as a short and long range attractor for cortical GABAergic interneurons during migration (43). Extracellular cues and signaling mechanisms that determine the spatial and temporal termination of cortical interneuron migration are emerging. Recent evidence suggests that factors secreted by pyramidal cells play important roles in guiding migrating interneurons (12). In addition, KCC2 influences the termination of interneuron migration into the neocortex through secretion of neuregulin 3 (24).

During development, the expression of the ion channels NKCC1 and KCC2 reverse, so that the initially high levels of NKCC1, a chloride importer, decrease, while levels of KCC2, a chloride exporter, increase. The relative levels of these membrane transport proteins determine the developmental switch of GABAergic interneurons from depolarizing (in young neurons) to hyperpolarizing (in mature neurons) (17; 18; 35; 65; 87). The expression of KCC2 during migration of interneurons correlates with the ability of these cells to respond to GABA as a stop signal, suggesting that KCC2 might act as a

switch controlling GABA from acting in a motogenic capacity to becoming a stop signal in migrating neurons (24). KCC2 also influences the final laminar position of interneurons reaching the neocortex (86). Manipulation of KCC2 expression and/or activity during development can therefore disrupt features of migrating neurons.

We previously observed that administration of MAM (methylazoxymethanol acetate) on embryonic day 33 (E33) induces KCC2 upregulation, which also reduces the speed and alters features of migrating neurons leaving the GE in the ferret (3). To determine if the migration defects directly relate to the increased levels of KCC2, we evaluate here the effect of KCC2 downregulation using BPA (2,2-bis-(4-hydroxy-phenyl) propane) and KCC2 antagonism (using the KCC2 antagonist VU0240551) on normal P0 cerebral cortex and on neocortex treated with MAM (which normally shows increased KCC2 levels).

Our findings indicate that exposure to environmental toxins such as BPA can affect brain development. We also show that an optimum expression and function of KCC2 is indispensable for the integrity of neuronal migration during corticogenesis in ferrets.

MATERIALS AND METHODS

Ethics Statement

All experiments in this work were done in accordance with the guidelines approved by the Institutional Animal Care and Use Committee (IACUC) at the Uniformed Services University of the Health Sciences (USUHS).

Animals and MAM Injection

Timed pregnant ferrets (Mustella putorius furo) were purchased from Marshall Farms (New Rose, NY). At embryonic day 33 (E33), pregnant ferrets were anesthetized with 5% isofluorane using a mask and given an intraperitoneal (IP) injection of methylazoxymethanol acetate (MAM, MRI Global, Kansas City, MO), at a dose of 14-mg/kg diluted in sterile 0.9% sodium chloride (Hospira Inc, Lake Forest, IL). MAM-treated pregnant jills were allowed to recover and gestation proceeded until 41 days when ferret kits are normally born. The total number of normal and MAM treated jills used is summarized in Table 1.

Preparation of Organotypic Slices

We prepared organotypic slice cultures as previously described (3; 93). Postnatal day 0 (P0) ferret kits were anesthetized with sodium pentobarbital (50 mg/kg, IP); when insensitive to pain, their brains removed and placed in ice-cold artificial cerebrospinal fluid (ACSF) composed of $NaCl^-$ (124 mM), KCl^- (3.2 mM), $CaCl^{+2}$ (2.4 mM), $MgCl^{+2}$ (1.2 mM), $NaHCO_3$ (26 mM), NaH_2PO_4 (1.2 mM), and 10 mM glucose and bubbled with 95% O_2 and 5% CO_2 under a laminar flow hood. Coronal slices (500 μm thick) were prepared from each hemisphere using a tissue chopper (Stoelting, Co., Wood Dale, IL, USA). Brain slices were transferred into 0.4 μm culture plate inserts (Millicell-CM, Bedford, MA, USA) placed in 6-well plates containing Minimum Eagles Medium, MEM, (GIBCO, Gaithersburg, MD) supplemented with 10% horse serum (GIBCO,

Gaithersburg, MD) and 4% G 1:2 (containing gentamycin and glutamine). Slices were incubated at 37°C under 5% CO2. The total number of kits is summarized in Table 1.

KCC2 Manipulation

BPA (Sigma Aldrich, St. Louis, MO) was dissolved in DMSO (Sigma Aldrich, ≥ 99%) to a concentration of 50nM with the DMSO final concentration being less than 0.01% in the medium as recommended by the manufacturer. The KCC_2 antagonist VU0240551 (Sigma Aldrich, St. Louis, MO) was added to the medium to a final concentration of 1μM or 5μM and added to the organotypic cultures. Our final concentration of DMSO was added to the medium alone and used in a set of organotypic cultures for western blots to determine its independent effect.

MEQ (6-Methoxy-*N*-Ethylquinolinium Iodide) Chloride Imaging

The MEQ chloride imaging was carried out according to standard protocol as previously described (21; 58; 113). The MEQ was reduced to a cell-permeable form, 6-methoxy-N-ethyl-1,2-dihydro- quinoline (DiH-MEQ), by dissolving 5 mg of MEQ in 0.1 ml of distilled water in a glass test tube placed under a stream of N2, and adding 12% sodium boratehydride ($Na_2B_4O_7 \cdot 10H2O$). The resulting solution was kept under a stream of N2 for 30 minutes until an oily yellow substance forms. Distilled water and ethyl acetate (0.5ml each) were then added to the reaction tube, vortexed and the solution allowed to separate into aqueous and organic layers. The organic layer (top) containing DiH-MEQ was carefully separated with a pipette and placed in a fresh tube. This step was repeated and the 2 organic layers combined and dehydrated by adding 100 mg of anhydrous magnesium sulfate ($MgSO_4$). After 5 minutes, the organic layer was transferred with a pipette into a glass microvial and the ethyl acetate evaporated with a stream of N2. DiH-MEQ was freshly prepared before each experiment and dissolved in 10ml ACSF immediately before dye loading. The slices, cut as described above, incubated for 30 minutes in the DiH-MEQ solution and allowed to absorb the dye. The initial florescence

(F0) intensity was recorded with a Zeiss 7 Multiphoton microscope equipped with Zen-2012 software (black edition). While recording continuously, the VU0240551 was added at 2 different times at a concentration of 1 μM or 5 μM and the fluorescence intensity (F) recorded. Graphs were plotted with normalizing fluorescence intensity by dividing by baseline F0 to compare the amplitude of change between cells. DiH-MEQ is quenched in the presence of chloride, thus a decrease in fluorescence corresponds to an increase in intracellular chloride concentration. The change in intracellular chloride concentration following KCC2 inhibition was estimated using the Stern-Volmer equation, as previously described (58; 70; 120). Our experiments were performed at 23oC and the Stern-Volmer constant for chloride ion at that temperature was estimated to be Kq = 16M-1 (58).

Western blotting

Treated organotypic slices were snap frozen on dry ice after 5 hours in culture (for VU0240551) and 24 hours (for BPA). For protein extraction, the frozen samples were thawed on ice and homogenized in ice-cold RIPA lysis buffer supplemented with sodium orthovanadate, protease inhibitors and PMSF (Santa Cruz Biotechnology, Dallas, TX). All homogenization was done by sonication at 4°C, followed by centrifugation at 4°C in an Eppendorf centrifuge 5415C at 20,000 rpm for 30 minutes. The supernatants were collected and protein concentrations determined using the bicinchoninic acid (BCA) protein assay method (Thermo Scientific, Pittsburgh, PA).

Protein samples were denatured by addition of Nupage SDS sample buffer and Nupage sample reducing agent (Invitrogen, Grand Island, NY) and heating at 70°C for 10 minutes. Electrophoresis of the cation-chloride transporter (KCC2) was accomplished using NUPAGE Novex 3-8% Tris-Acetate gel and NUPAGE Tris-Acetate SDS running buffer supplemented with NUPAGE antioxidant (Invitrogen, Grand Island, NY) and 40μg of protein loaded in each well. Proteins were transferred onto 0.45 μm-pore nitrocellulose membranes using the iBlot dry blotting system (Invitrogen, Grand Island,

NY). Membranes were blocked for 1 hour at room temperature in 5% milk blocking buffer dissolved in 1X TBS supplemented with 0.1% Tween-20 (Bio Rad, Hercules CA) and incubated with rabbit polyclonal anti-KCC2 (1:500, Millipore, Billerica, MA), at 4°C overnight. The next day, membranes were washed repeatedly in TBS-Tween solution and incubated in goat anti-rabbit secondary antibody conjugated to horseradish peroxidase (Invitrogen, Grand Island, NY, 1:2000) diluted in TBS-Tween, followed by detection using enhanced chemiluminescence reagents (PerkinElmer, Melville, NY). The bands were quantified using ImageJ software (https://imagej.nih.gov/ij/) and the densities compared across different conditions using a one-way or two-way-ANOVA (as needed) followed by the Tukey or Sidak post-hoc multiple comparison tests as needed.

Cell Labeling

We used electroporation to focally transfect cells within the ventricular zone (VZ) in vitro as described previously (3). Transfection was accomplished using a plasmid that codes for red fluorescent protein (RFP), which was cloned into pCAGGS expression vector (a gift from Dr. Tarik Haydar). Between 4 and 5 μL of plasmid DNA (1 – 2 μg/μL) was injected onto the GE surface of the organotypic slices. The cathode of a gene paddle electrode (Harvard Apparatus, Inc., Holliston, MA, USA) was placed within the lateral ventricle close to the VZ of the GE while the anode was positioned close to the pial surface in an appropriate position. A pulse of 60 V was applied 4 times, each for 50 ms at intervals of 950 ms using a BTX ECM830 pulse generator (Harvard Apparatus, Inc., Holliston, MA, USA) (45). Slices were incubated as above for at least 24 hours prior to video imaging.

Video Imaging

After incubating the organotypic slices for 24-48 hours, migrating neurons were continuously visualized using an Axiovert 200 inverted microscope fitted with an apotome and Axiovision software (Carl Zeiss AG, Oberkochen, Germany). The

microscope was also fitted with an incubation chamber and a holder for the slices, which were maintained with humidification at 37°C and 5% CO2. Serial stacks of images taken through the thickness of the slice were collected using a ×10 objective every 30 min for 24 hours using Zen software (black edition). The image stacks were collapsed into a single frame prior to analysis of migration. Migrating cells leaving the GE were analyzed after crossing the corticostriatal boundary into the neocortex.

Analysis of Migration

To measure speed, we tracked migrating cells captured in real time using the M-trackJ plugin of the FIJI package of imageJ software (https://imagej.nih.gov/ij/). The initial data captured included the tracked distances, the travel time, the speed of movement and the angles of turn of neurons. These data were extracted and analyzed using Graph Pad Prism version 6 software. A student's t-test was used to compare two (2) means and a one-way or two-way analysis of variance (ANOVA) followed by a Tukey post hoc test was applied to compare 3 or more means and differences evaluated at $p < 0.05$.

RESULTS

Cell labeling and migration

In brains with increased levels of KCC2, interneurons migrating into the cerebral cortex move more slowly and show lowered amounts of exploratory behavior (Abbah and Juliano 2014; Abbah et al 2014). To test whether this abnormal behavior is specifically due to the presence of increased KCC2, we used two methods to reduce the activity of this chloride transporter protein. We used the same cell labeling technique (in vitro electroporation) as previously described, to visualize and track migrating interneurons leaving the GE toward the neocortex (3). Figure 14 shows electroporated cells in an organotypic slice that are migrating en route to the neocortex, in a normal ferret (Figure 14A) and in MAM-treated ferret (Figure 14B).

KCC2 downregulation with bisphenol A (BPA) and its effect on features of migrating interneurons leaving the GE

The effect of BPA on brain development and function is substantial (90). BPA downregulates KCC2 mRNA and protein levels in neurons (132). Gestational E33 MAM treatment upregulates KCC2, which correlates with decreased speed and altered migratory features of interneurons leaving the GE (3). Concentrations of 50nM and 100nM of BPA reduce KCC2 levels in cultured neurons or organotypic cultures (132). We initially observed that 50 nM BPA supported optimal viability of neurons in slices, while 100 nM induced a level of toxicity so that the slices appeared unhealthy after 24 h in culture. As a result, to test the causality between KCC2 levels and the speed of migrating neurons, we treated organotypic cultures with 50 nM BPA. Since KCC2 slows the speed of migrating interneurons (24), we predicted that a decrease in KCC2 levels would increase the speed of migrating neurons in our preparation. BPA reduces KCC2 levels by increasing KCC2 gene methylation and consequently the methyl-CpG-binding protein 2 (MECP2) (132). To initially determine the effect of BPA on levels of KCC2 we conducted western blots on the tissue taken from the organotypic cultures treated with

BPA or with vehicle (medium + DMSO) after 24 hours. BPA treatment decreases KCC2 protein levels significantly compared to control but DMSO alone has no detectable effect on KCC2 protein levels (Figure 15A & B). We next studied the effect of BPA on the migratory speed of neurons leaving the ganglionic eminence. After adding 50 nM of BPA to the medium of prepared slices, each cultured slice received electroporation into the GE with RFP. Following incubation for 24 hours, we imaged each slice for an additional 24 h at 30-minute intervals. This analysis over the 24 h of migration showed a significant increase in the speed and step size of migrating neurons from the normal cultures treated with 50 nM BPA compared to control (Figure 15C & E). When the slices treated with E33 MAM were evaluated, we found the migration speed of those receiving BPA to be significantly increased (Figure 15D & F).

Movie 1 shows the migration behavior of control neurons. Cells can be seen moving with an overall trend toward the neocortex, but migrating neurons travel in multiple directions and show turns in unique trajectories. Our previous studies revealed that organotypic slices receiving MAM treatment (producing increased levels of KCC2), show decreased numbers of turns as the neurons move toward the neocortex (Abbah and Juliano 2014). As we see in Figure 15A and B that treatment with BPA reduces KCC2, we assessed the number of turns made by migrating cells in control cultures and those treated with BPA. To measure the turns, we used a "track changes" plugin in Fiji (ImageJ) to reveal the path of cells as they moved. Movie 2 indicates the path of individual cells as they traveled in control slices. Each turn was measured when a cell changed in path of movement by at least 30 degrees. BPA treatment significantly increases the number of turns made by neurons per hour in the course of migration compared to control (Figure 15G) and this is also true for E33 MAM slices treated with BPA (Figure 15H). Movie 2 indicates the paths of neurons in a control slices and the turns made; Movie 3 shows the tracks of neurons migrating in BPA treated slices.

Overall, we find that adding BPA to organotypic cultures reduces KCC2 levels and the speed and behavior of cells migrating away from the ganglionic eminence.

Validation of KCC2 antagonist (VU0240551) using MEQ chloride imaging

KCC2 inhibition was achieved by application of the antagonist VU0240551 and confirmed with the MEQ chloride imaging. The KCC2 antagonist VU0240551 selectively and specifically inhibits KCC2 by binding competitively to the K^+ site and non-competitively to the Cl^- site in the KCC2 active region thereby hindering chloride flux. Various methods successfully demonstrate KCC2 inhibition by this antagonist (34; 36). To verify that VU0240551 blocked Cl^- movement, we used MEQ chloride imaging on slices similar to those used to study migration. In the MEQ chloride imaging shown in Figure 16, the fluorescence is quenched by chloride ions entering the cell, resulting in an inverse relationship between intracellular [Cl^-] and fluorescence intensity. Higher fluorescence intensity in a given cell corresponds to a lower intracellular [Cl^-] and vice versa. Figure 16A shows neocortical neurons filled with the dye MEQ; Figure 16B & C indicates there is no bleaching of the dye because after 15 minutes of recording, the fluorescence intensity does not diminish. Figure 16C presents a magnification of the area imaged for 15 minutes outlined with the red square in Figure 16B. Application of the KCC2 antagonist at 1 μM and 5 μM concentrations decrease the fluorescence intensity indicating an increase in intracellular [Cl^-], which restores when the antagonist is washed out (Figure 16D). We estimated the change in intracellular chloride concentration using the Sterm-Volmer equation; the results shown in Figure 16E reveal a ~10mM increase in intracellular chloride concentration corresponding to the change in fluorescence intensity in Figure 16D. We estimated the increase in intracellular chloride concentration in 16 neurons and plotted their values and the average change (Figure 16F). The increase in intracellular chloride concentration varied between 3.1-10.5 mM with an average of 6.0 mM ± 0.5 (SEM). The fluorescence intensity during application of the antagonist was

normalized to baseline recording (without the antagonist) so that each cell served as its own control (before and after treatment with the antagonist) as shown in Figure 16D.

Effect of KCC2 inhibition on features of migrating neurons leaving the GE

After successful inhibition of KCC2 protein activity in organotypic slices we evaluated the migratory behavior of inhibitory neurons using live imaging. Under certain circumstances (not fully understood) KCC2 can be degraded through calcium activated protease calpain and it is possible that long term inhibition of KCC2 by its antagonist VU0240551 could lead to degradation of the KCC2 protein (34; 102). In order to ensure the integrity of KCC2 protein in the organotypic cultures we conducted western blots five hours after treatment of the organotypic slices with the KCC2 antagonist. Our choice of 5 hours for the treatment was informed by previous findings that the MEQ dye stayed inside the cell up to 4 hours (58). Figure 17A & B show the antagonist has no effect on KCC2 protein levels after 5 hours of incubation. Analysis of live imaging of the slices treated with 5μM KCC2 antagonist for 5 hours shows an increase in the average speed as well as the average step size of cells leaving the GE as shown in Figure 17C & E. The increase in migration speed is also significant for the E33 MAM slices treated with the KCC2 antagonist (Figure 17D & F). Movie 4 shows the migration behavior of neurons in slices treated with the KCC2 antagonist.

Variability of speed of migrating neurons over time

Movie 1 shows that interneurons leaving the ganglionic eminence move in multiple directions and they often make turns. Some cells also move for a time and then remain in the same place without a specific direction (see Movie 4). Our assessment of migratory speed focused entirely on the time during which the cells moved without including the times they stopped and explored the environment. We find that with treatment of BPA and the KCC2 antagonist the average speed of cells leaving the GE increases overall. Because substantial unevenness in the overall pattern of movement

occurs, we assessed cells that moved continuously over a period of 5 hours and evaluated the average speed variability over time. We computed the average speed across the time frames and focused on neuronal migration for this time block because we know the KCC2 antagonist does not degrade KCC2 protein levels for at least 5 hours of treatment (Figure 17 A & B). Figure 18A and B show the speed-time graphs for BPA and KCC2 antagonist treatment. Figure 18A shows that the migration speed of neurons treated with BPA generally exhibits a gradual increase over the period studied, but displays some variability over the 5 hour period. The speed of the BPA treated neurons is typically significantly higher than that of control neurons at all time points except between the 2 and 3rd hour. Figure 18B shows that after treatment with the KCC2 antagonist, the migration speed increases gradually until the 3rd hour of migration and then decreases slightly, while remaining significantly greater than the control migration speeds until the last time point.

Summary of findings

Neuronal migration is intricately fine-tuned by a myriad of factors (both internal and external) to attain the normal cytoarchitecture needed for proper function of the brain (42; 79; 81; 83). We reported earlier that gestational delivery of MAM (an environmental toxin) on E33 upregulates KCC2 protein, which correlates with decreased speed and altered behavior of migrating interneurons leaving the GE in ferret neocortex (3). Here we show that downregulation of KCC2 through another environmental toxin (BPA) and a KCC2 antagonist counteracts the abnormal features of neuronal migration observed after increases in KCC2.

BPA treatment in organotypic slices at a dose of 50 nM for 24 hours significantly downregulates KCC2 protein to result in increased speed and step size of migrating interneurons leaving the GE compared to control migrating neurons. Similarly, treatment of organotypic slices with 1 μM and 5 μM of the KCC2 antagonist VU0240551 inhibits KCC2 activity by limiting chloride flux. This also correlates with increased speed and

step size of migrating neurons. Reducing the effect of KCC2 (with BPA or an antagonist) tends to counteract the effect of MAM treatment and increases the migration speed.

DISCUSSION

KCC2-NKCC1

The molecular mechanisms regulating the initiation, progress and termination of neuronal migration are numerous. The balance between excitation and inhibition in the neocortex is partially controlled by the KCC2-NKCC1-GABAergic system; NKCC1 is initially high, resulting in chloride import, which is eventually replaced by increased levels of KCC2, resulting in chloride export. This arrangement initially acts as a motogenic signal, encouraging neurons to move, and eventually as a stop signal, with the rise of KCC2, marking the termination of cortical migration (24). Developmental manipulation of this system assists in understanding the role of these ion channel proteins in the progress and termination of cortical migration. KCC2 manipulation specifically influences GABA function during development and particularly affects cortical migration (3; 24; 32; 60). The developmental switch that results in the transformation of GABA from excitatory to inhibitory, due to changes in the ratio of KCC2 and NKCC1 is crucial to understanding neuronal development (24). A precocious overexpression of KCC2 accelerates the perinatal chloride shift, which consequently slows down the speed of migrating neurons and eventually makes them pause (24). In our model, gestational E33 MAM treatment causes an early upregulation of KCC2 that correlates with decreased speed as well as altered behavior of migrating interneurons in ferret neocortex (3).

KCC2 downregulation with BPA increases the speed and step size of migrating interneurons leaving the GE.

BPA is an estrogenic chemical used in making polycarbonate and epoxy resins lining food and beverage cans and bottles. It belongs to the bisphenol family of compounds comprising, but not limited to, bisphenol B, C, E, and F. BPA is a potential gene toxicant during embryonic development and exposure can result in diverse adverse effects on human and animal health. These incorporate wide-ranging effects that include isolation behavior of babies from mothers in non-human primates as well as reduced

overall exploration of their environment (88). Other experiments report endocrine disruptions leading to obesity (121) and decreased fertility and fecundity in CD-1 mice (25). More directly related to neuronal development, several studies report abnormal cortical development when pregnant animals receive BPA during gestation. Relevant findings include acceleration of corticogenesis and an altered laminar pattern (59; 67; 68). These direct effects on the cerebral cortex may be a direct result of the increased migratory speed we see in our current study.

Both prenatal and in-vitro exposure of neurons to BPA downregulate KCC2 mRNA and protein through epigenetic modifications, thereby delaying the KCC2 driven perinatal chloride shift and consequently increasing the speed of migrating interneurons in the neocortex (132). This agrees with our finding that BPA treatment downregulates KCC2 and consequently increases the speed of migrating neurons leaving the GE in ferret neocortex. We also show that migrating neurons treated with BPA increase their step size as compared to control. Increased speed and step size implies movement over a longer distance than normal, which in terms of neuronal migration could lead to misplacements of neurons (cortical dysplasia) and consequent abnormal function of the brain. Our findings reveal that the perinatal chloride shift controlled by KCC2 is an important component influencing the speed and pattern of migrating neurons. Generally migrating neurons slow down and eventually stop moving when they differentiate and mature to assume the right position for normal function. The delay in perinatal chloride shift (caused by BPA treatment in our case) may delay the maturation time window and also maintains the GABAergic system in a depolarized state favorable for neuronal motility through calcium mediated activation of the cytoskeleton (through the voltage sensitive calcium channels, VSCC) in the normal slices (16; 24; 55). The increase in speed and step size may be suggestive of a stronger depolarization effect leading to accentuated calcium mediated activation of the cytoskeleton through the VSCC, pending further investigations. In the case of the MAM treated slices, treatment with BPA

provides and influence that suggests a reversal of the effect of MAM, resulting in increased migration speed than when treated with MAM alone. We found earlier that E33 MAM treated neurons were less exploratory by making fewer turns than controls (3) indicating that abnormal KCC2 upregulation in our model probably impeded the cues, sense of orientation, and direction of migrating neurons. Our current finding shows that BPA treatment significantly increases the number of turns made by migrating neurons per hour compared to control. This suggests that KCC2 may play a role in neuronal guidance during migration as well (76).

The action of BPA in KCC2 downregulation occurs through epigenetic modification (methylation) of the KCC2 gene (132). This global mechanism may not be specific to KCC2 and could possibly affect the expression of other genes involved in regulating neuronal migration. We are therefore cautious not to attribute the alterations in features of migration solely to KCC2 downregulation since other unknown players could be involved. As a result, we evaluated the effect of manipulating KCC2 levels with a pharmacologic antagonist.

Inhibition of KCC2 activity by the antagonist VU0240551

The use of VU0240551 enabled us to specifically inhibit the activity of KCC2 without affecting NKCC1 and other anion channels, thereby enabling assessment of the specific effect of reducing KCC2 activity on features of migrating neurons. This KCC2 antagonist VU0240551 selectively inhibits KCC2 by binding competitively to the K+ site and non-competitively to the Cl- site in the KCC2 active region and impairing chloride movement (34; 36). This manipulation in our hands, resulted in an increase in intracellular chloride concentration ranging from 3.1-10.5 mM. Given the physiologic levels of intracellular chloride concentration in neurons is about 4mM, we are confident the estimated increase (~2-2.5 fold) is enough to alter KCC2 activity reflected in the variation of migration speed and step size. Here again, we show that inhibition of KCC2 activity correlates with an increase in speed and step size of migrating neurons leaving

the GE, suggesting that interference with KCC2 alters neuronal migration. Blocking chloride channels delays the rate of chloride extrusion, which may delay the GABA polarity switch leading to an increase in speed and step size of migrating neurons most likely through the VSCC. Application of the KCC2 antagonist to E33 MAM slices significantly increases the average speed over that of MAM treated slices alone. It is clear that inhibiting the activity of KCC2 (either by BPA, which reduces the production of KCC2 protein, or by a specific pharmacologic antagonist) increases the speed of migrating neurons and also restores at least some exploratory behavior.

VARIABLE SPEED OF MIGRATING NEURONS OVER TIME

The speed of migrating neurons for both normal slices and those treated to decrease KCC2 tends to increase over the initial 5 hours of recording. Since these values represent the average of all the cells we measured, obvious variability occurred among neurons. In addition, we only measure those cells that were moving continuously for 5 hours, many neurons moved intermittently. Nevertheless, the overall trend for moving neurons shows increased speed. This suggests that the migrating cells are healthy and not adversely affected by being in culture or under the drug treatment. It is not clear why the speed increases over this period of time but it may represent a decrease in conflicting signals present in the organotypic culture. In addition, the speed of the neurons in slices treated with BPA and the KCC2 antagonist is generally increased from the time we began evaluating their movements. There are some time points that show decreases in the average speed but these are mostly likely due to the overall variability of response. It is not clear what factors account for the observed pattern of variability of the speed in this case and understanding of the detailed mechanisms requires further investigations.

CONCLUSION

The KCC2 is a chloride exporter and NKCC1 is a chloride importer. In young neurons, the expression of NKCC1 is higher relative to KCC2 leading to a greater

intracellular chloride concentration making GABA depolarizing. As the neurons mature, the expression of KCC2 becomes increased relative to NKCC1, leading to a higher extracellular chloride concentration making GABA hyperpolarizing. The switch of GABA polarity from depolarizing to hyperpolarizing is precisely regulated by the balance of KCC2 and NKCC1, which contributes to factors regulating motility of migrating interneurons in the cortex. The switch in GABA polarity influences the motility of migrating neurons by stimulating the cytoskeleton through the VSCCs. A precocious upregulation of KCC2 through MAM treatment may hasten the polarity switch to hyperpolarization, which slows down neuronal motility, whereas a precocious downregulation of KCC2 through pharmacologic treatment delays the polarity switch extending depolarization, which may stimulate neuronal motility.

Figure 6 shows a cartoon of KCC2 manipulation in our experiments. A shows that under normal conditions, the balance of KCC2 and NKCC1 results in a migration pattern that where neurons migrate at a normal speed and reach the right destination at the right time. B represents KCC2 downregulation by BPA treatment. Under this condition, decreased KCC2 protein is produced and reduces that overall amount of available KCC2 leading to a delay in the polarity switch causing a longer depolarization time window and stimulating neuronal motility. In C, a deficiency in the overall activity of KCC2 protein due to inhibition by the KCC2 antagonist (VU0240551) exists and leads to a reduction in chloride ion export causing a delay in polarity switch and consequent stimulation of neuronal motility. D represents regulation of neuronal motility under MAM treatment where precocious KCC2 upregulation hastens the GABA polarity switch and slows migrating neurons. E shows regulation of neuronal motility under MAM treatment followed by BPA or the KCC2 antagonist. Here, BPA and the KCC2 antagonist counteract the effect of MAM by restoring the speed and behavior of migrating cells.

Both KCC2 downregulation and interference with KCC2 activity have a similar effect on migrating neurons. The BPA downregulates KCC2 expression leading to fewer

KCC2 molecules whereas the antagonist blocks normal function reducing overall KCC2 activity. The BPA acts longer and affects gene expression, whereas the KCC2 antagonist is target specific and more focal, causing a more succinct functional outcome.

The use of MAM, on one hand, and BPA and VU0240551 on the other, are both cases of KCC2 manipulation indicating that an alteration in the perinatal chloride shift during brain development leads to abnormal neuronal migration. Although these are not therapeutic agents, we believe our findings serve to enhance further research with KCC2 and its expression and functional machinery as molecular targets in abnormal neuronal migration.

Conflict of Interest

None declared.

Funding

This research was funded by PHS NS 24014; DOD – USUHS - RO703041.

Acknowledgements

We thank all members of the Laboratory Animal Medicine (LAM) who helped us with excellent animal care especially Maj. Maxwell, Maj. Reiter, Sgt. Aguilla and Sgt. Fluid. We also thank Dr. Dennis McDaniel for his assistance with some of the live imaging experiments and Mitali Chatterjee for general assistance with experiments.

Table 4: Number of normal ferret kits used for slice culture and live imaging experiments.

Jills	Number of kits used	Treatments
F1 Normal	1 P0 kit	Control (medium), Vehicle (medium +DMSO) on different slices
	1 P0 kit	Treated with BPA (50nM and 100nM)
	2 P0 kits	Treated with KCC2 antagonist (1μM and 5μM)
F2 Normal	1 P0 kit	Control, Vehicle, BPA-50nM and 100nM, KCC2 antagonist 1μM, and 5μM.
	1 P0 kit	Control, Vehicle, BPA-50nM and 100nM KCC2 antagonist 1μM, and 5μM.
	1 P0 kit	Control, Vehicle, BPA-50nM and 100nM, KCC2 antagonist 1μM, and 5μM.
	1 P0 kit	Control, Vehicle, BPA-50nM and 100nM, KCC2 antagonist 1μM, and 5μM.
F3 Normal	1 P0 kit	Control, Vehicle, BPA-50nM, and KCC2 antagonist 5μM.
	1 P0 kit	Control, Vehicle, BPA-50nM, and KCC2 antagonist 5μM.
	1 P0 kit	Control, Vehicle, BPA-50nM, and KCC2 antagonist 5μM.
	1 P0 kit	Control, Vehicle, BPA-50nM, and KCC2 antagonist 5μM.
F4 Normal	1 P0 kit	Control, Vehicle, BPA-50nM, and KCC2 antagonist 5μM.
	1 P0 kit	Control, Vehicle, BPA-50nM, and KCC2 antagonist 5μM.
	1 P0 kit	Control, Vehicle, BPA-50nM, and KCC2 antagonist 5μM.
	1 P0 kit	Control, Vehicle, BPA-50nM, and KCC2 antagonist 5μM.
F4 Normal	1 P0 kit	Control, Vehicle, BPA-50nM, and KCC2 antagonist 5μM.
	1 P0 kit	Control, Vehicle, BPA-50nM, and KCC2 antagonist 5μM.
	1 P0 kit	Control, Vehicle, BPA-50nM, and KCC2 antagonist 5μM.
	1 P0 kit	Control, Vehicle, BPA-50nM, and KCC2 antagonist 5μM.
F5 Normal	1 P0 kit	Control, Vehicle, BPA-50nM, and KCC2 antagonist 5μM.
	1 P0 kit	Control, Vehicle, BPA-50nM, and KCC2 antagonist 5μM.

	1 P0 kit	Control, Vehicle, BPA-50nM, and KCC2 antagonist 5μM.
	1 P0 kit	Control, Vehicle, BPA-50nM, and KCC2 antagonist 5μM.
F6 E33 MAM	1 P0 kit	Control, Vehicle, BPA-50nM and 100nM, KCC2 antagonist 1μM, and 5μM.
	1 P0 kit	Control, Vehicle, BPA-50nM and 100nM, KCC2 antagonist 1μM, and 5μM.
	1 P0 kit	Control, Vehicle, BPA-50nM and 100nM, KCC2 antagonist 1μM, and 5μM.
	1 P0 kit	Control, Vehicle, BPA-50nM and 100nM, KCC2 antagonist 1μM, and 5μM.
F7 E33 MAM	1 P0 kit	Control, Vehicle, BPA-50nM, and KCC2 antagonist 5μM.
	1 P0 kit	Control, Vehicle, BPA-50nM, and KCC2 antagonist 5μM.
	1 P0 kit	Control, Vehicle, BPA-50nM, and KCC2 antagonist 5μM.
	1 P0 kit	Control, Vehicle, BPA-50nM, and KCC2 antagonist 5μM.
F8 E33 MAM	1 P0 kit	Control, Vehicle, BPA-50nM, and KCC2 antagonist 5μM.
	1 P0 kit	Control, Vehicle, BPA-50nM, and KCC2 antagonist 5μM.
	1 P0 kit	Control, Vehicle, BPA-50nM, and KCC2 antagonist 5μM.
	1 P0 kit	Control, Vehicle, BPA-50nM, and KCC2 antagonist 5μM.

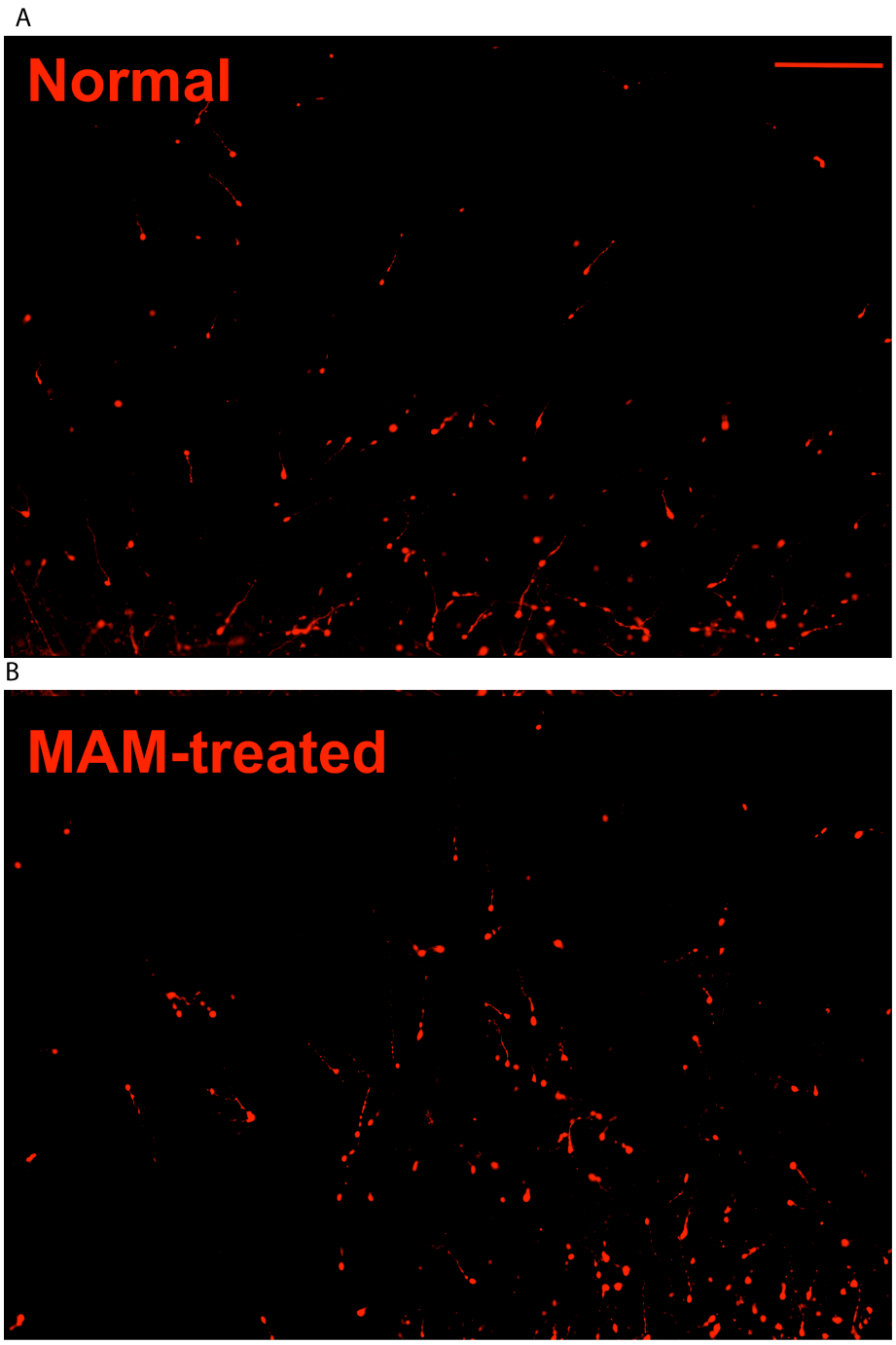

Figure 14: Electroporated slices showing migrating neurons

Electroporated neurons in organotypic slices expressing RFP enhanced by immunohistochemistry. (A): RFP expressing neurons in the GE of a normal ferret slice. (B): RFP expressing neurons en route to the neocortex in the GE of MAM-treated ferret slice. Scale: 200μm for A and C; 50μm for B and D.

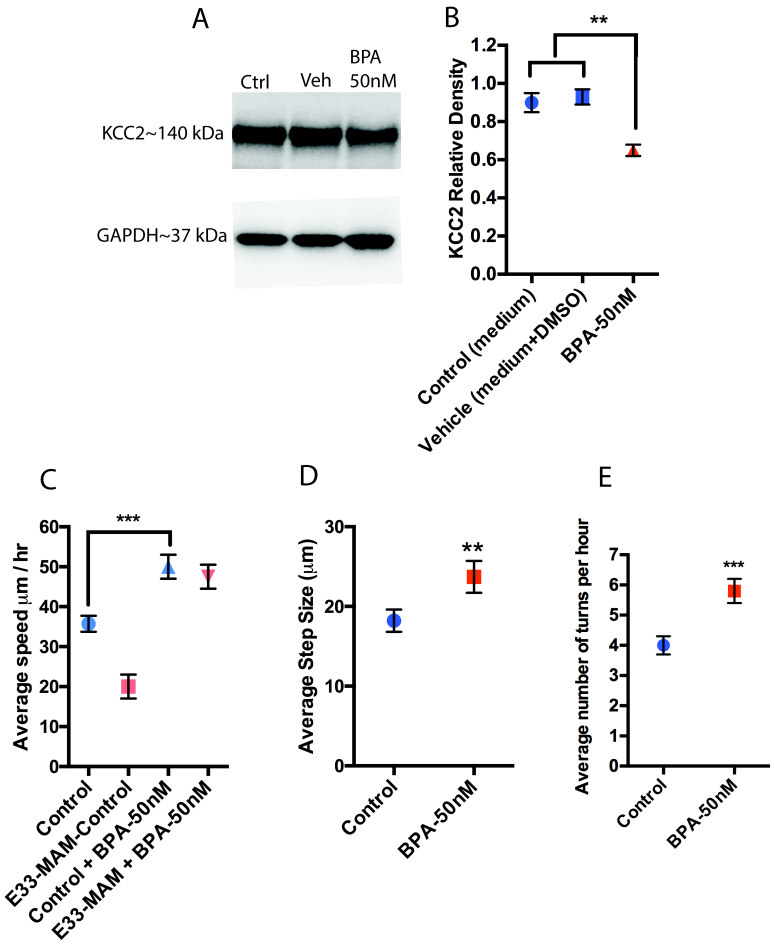

Figure 15: BPA treatment decreases KCC2 protein levels and increases features of migrating neurons.

(A) and (B) BPA treatment for 24 hours significantly decreases KCC2 protein levels ANOVA F (2, 6) = 14.18, n=3 animals in each group, followed by a Tukey post hoc test, ** $p < 0.01$. **(C):** BPA treatment (50 nM) increases the speed of migrating neurons significantly in normal ferret organotypic cultures; ANOVA F (3, 224) = 7.3, *** $p < 0.001$. Although the migrating neurons in the MAM treated cultures also show an increase in the speed, the numbers were low. **(D):** BPA treatment significantly increases the step size of migrating neurons in normal ferrets, Student's t-test, ** $p < 0.01$. **(E):** BPA treatment significantly increases the number of turns, student's t-test ***$p < 0.001$. N = 130 neurons (Control), 87 neurons (Control + BPA-50nM), 5 neurons (E33-MAM-control), and 6 neurons (E33-MAM + BPA).

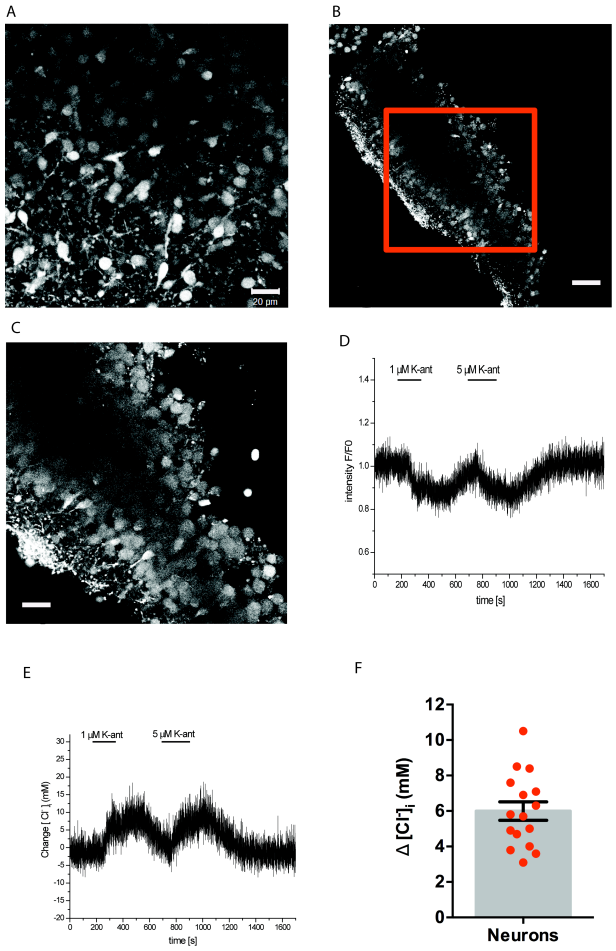

Figure 16: MEQ chloride imaging

(A) Neurons filled with MEQ dye in organotypic slices. **(B)** The intensity of fluorescence remains intact after 15 minutes of recording (without drug treatment) and shows no bleaching or leakage of dye. The image contained in the red box is shown magnified in **(C). (D)** A representative trace of fluorescent recording indicates a drop in intensity after antagonist application and recovery after washing out the drug. Slices were treated with 1µM and 5µM of VU0240551. This trace demonstrates inhibition of the KCC2 activity via the antagonist VU0240551 leading to transient increased intracellular [Cl^-], and subsequent quenching of MEQ fluorescence intensity. **(E):** Estimated increase in intracellular chloride concentration corresponding to the decrease in fluorescence intensity in **(D). (F):** Scatter plot (red dots) and average plot (gray bar) of estimated increase in intracellular chloride concentration in neurons varying between a minimum value of 3.1 to a maximum of 10.5 mM with an average of 6.0 mM ± 0.5. N = 16 neurons, 2 slices (10 neurons from one slice and 6 neurons from another slice), 2 animals (one slice from each animal). Scale = 20µm for A and C and 50µm for B.

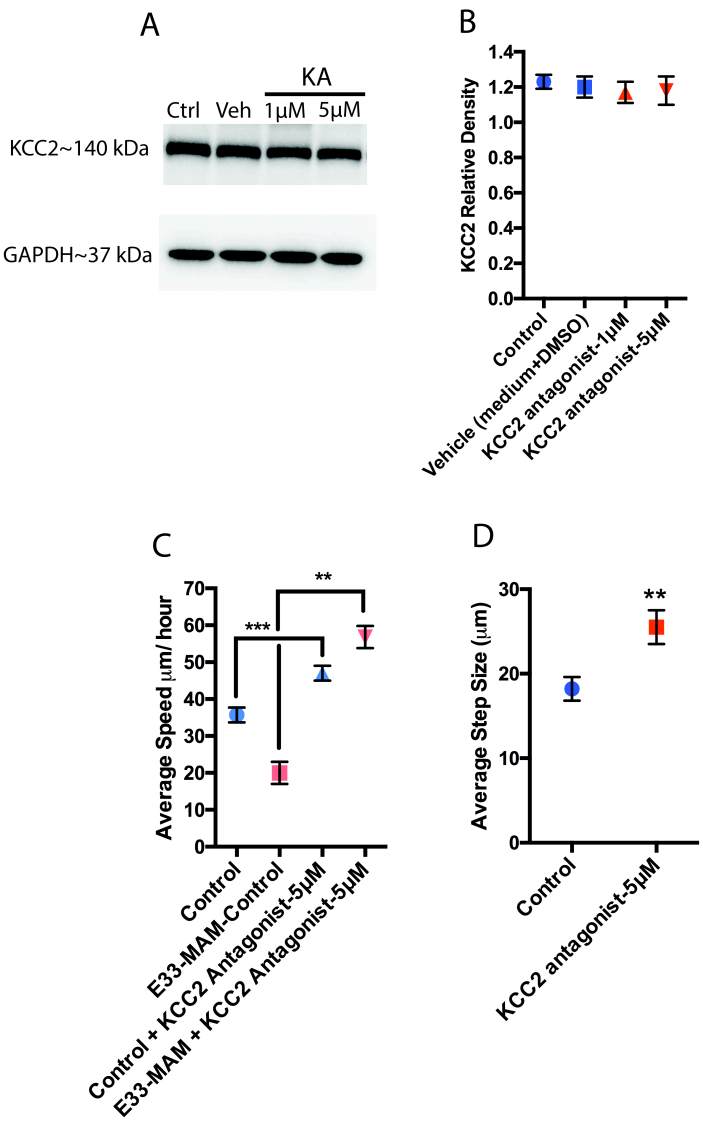

Figure 17: KCC2 antagonist treatment increases features of migrating neurons with no effect on KCC2 protein levels.

(A and B) Treatment of organotypic slices with VU0240551 for 5 hours has no significant effect on KCC2 protein levels; n = 3 animals for each group. Also included is a set of slices incubated with DMSO to determine its direct effect on the cultures. **(C)** Treatment of organotypic slices with VU0240551 significantly increases the speed of migrating neurons in both normal and E33 MAM treated ferrets. Speed data extracted for the first 5 hours of neuronal migration; ANOVA F (3, 262) = 11.14, ** $p < 0.01$. **(D)** Treatment of organotypic slices with VU0240551 increases the step size of migrating neurons in normal ferrets significantly for the first 5 hours, student's t-test, ** $p < 0.01$. N=80 neurons (Control), 63 neurons (Control + KCC2 antagonist), 5 neurons (E33 MAM Control), 22 neurons (E33 MAM + KCC2 antagonist).

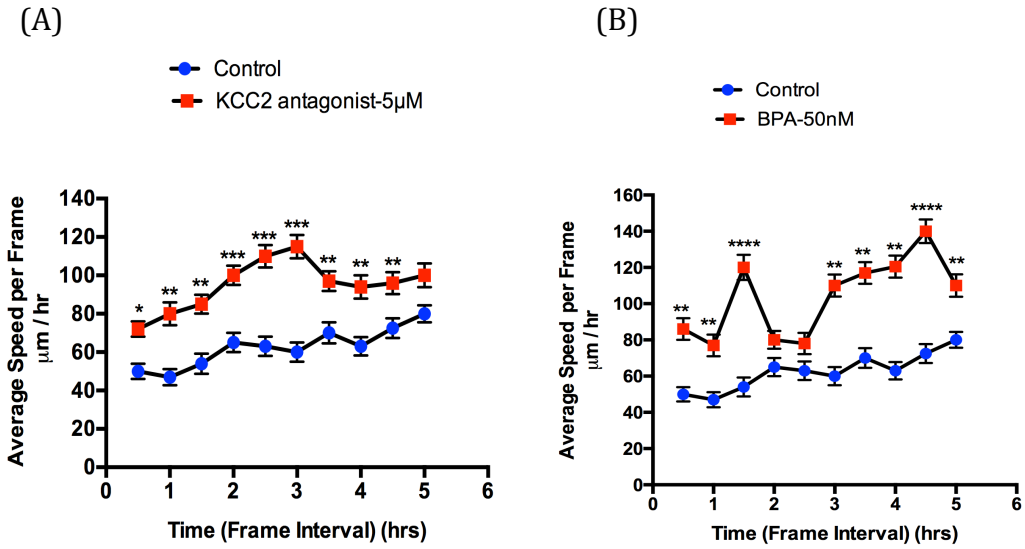

Figure 18: Variation of migration speed during the first 5 hours of the migration assay.

(A) When 5 μm of the KCC2 antagonist, VU0240551 is added to the culture medium, the speed of migration increases gradually from the onset up to 3 hours and then decreases in the next ½ hour and remains fairly constant until the 5th hour. The migration speed for neurons in the slices treated with the KCC2 antagonist is significantly higher than that of control values at all time points except for the last data points collected at the top of the 5th hour. Plotted here are the average values for all the time points across the first 10 frames corresponding to the first 5 hours of neuronal migration. 2-Way ANOVA, Row Factor, F (9, 1520) = 7.9 followed by Sidak Post hoc test, * $p < 0.05$, *** $p < 0.001$, **** $p < 0.0001$. **(B)** After BPA treatment, the migration speed generally increases for both the treated and control cells, with several fluctuations. The migration speed under BPA treatment is significantly higher than that of control at all time points except at 2 and 2.5 hours; 2-Way ANOVA, Row Factor F (9, 1460) = 13.6 followed by Sidak post hoc test ** $p < 0.01$, **** $p < 0.0001$. N = 80 neurons for Control, 63 neurons for KCC2 antagonist and 38 neurons for BPA.

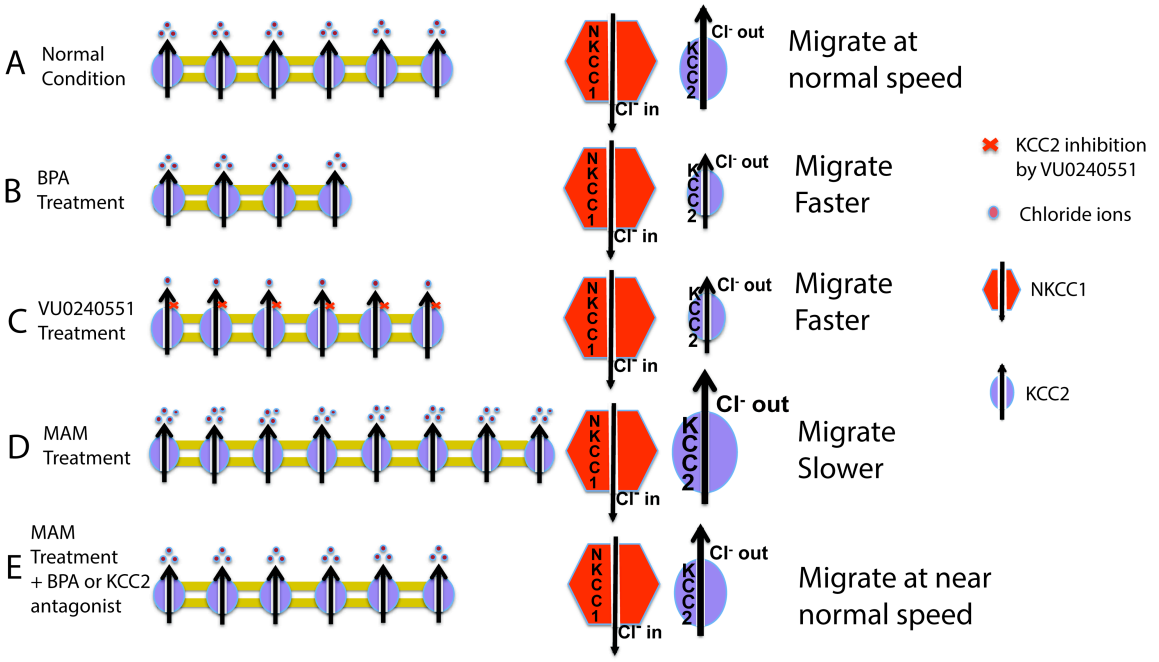

Figure 19: Model of KCC2 manipulation

(A) Normal condition: Early in migration, NKCC1 expression is higher than KCC2. This makes GABA depolarizing and drives migration at normal speed. **(B)** After BPA treatment KCC2 expression reduces leading a decrease in its activity. Depolarization prevails longer and this stimulates motility and increases migration speed. (C): After VU0240551 treatment KCC2 channels are blocked, reducing its activity and causing a longer depolarization leading to increased speed of migration. (D): MAM treatment increases KCC2 expression reducing the GABA depolarizing effect and slowing down migrating neurons. **(E):** Adding BPA or KCC2 antagonist to MAM treated slices tends to counter the effect of MAM and restore the migration speed at near normal speed.

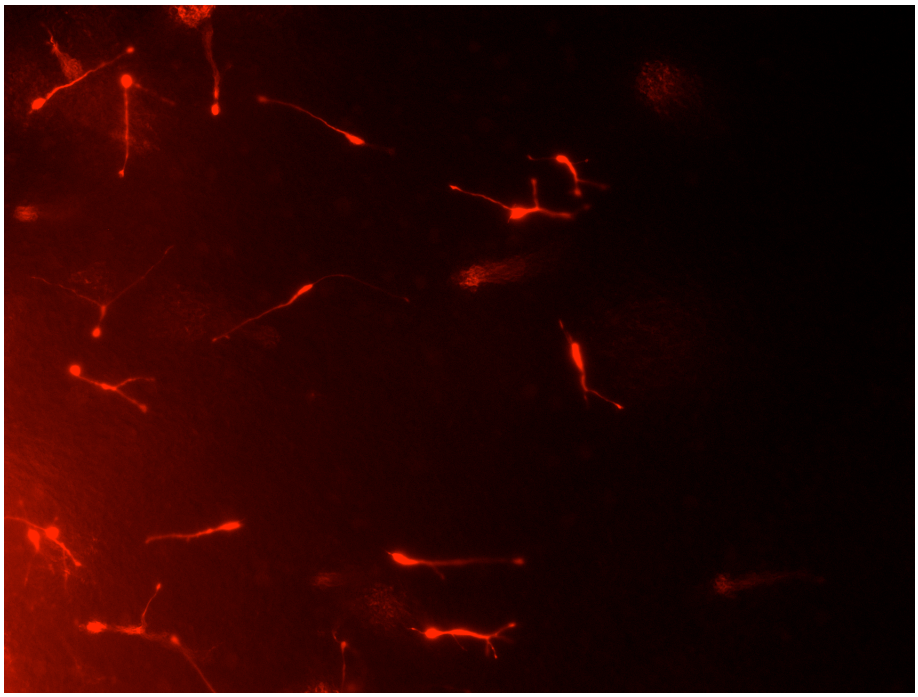

Movie 1: Migrating neurons leaving the GE in a normal (control) slice.
Neurons leaving the GE neurons and travelling towards the neocortex are guided by the leading process and display exploratory behaviors such as turning, giving out and retracting processes, changing direction and pausing.

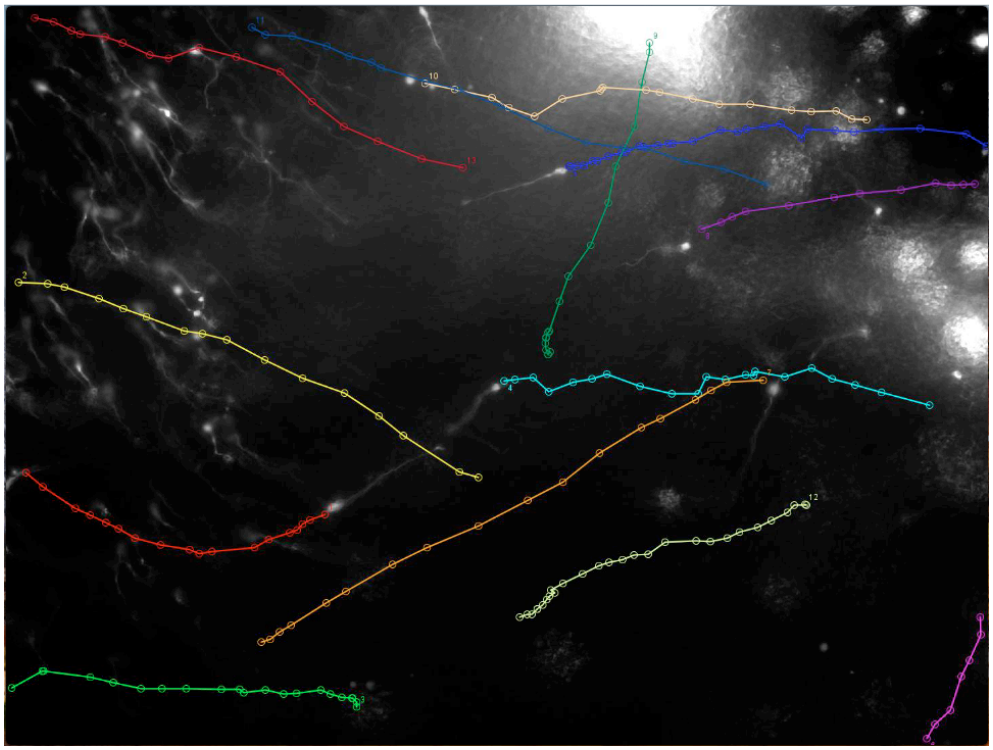

Movie 2: Tracks of migrating neurons showing turns in a control slice.
The tracks show less turns compared to movie 3 (BPA treated).

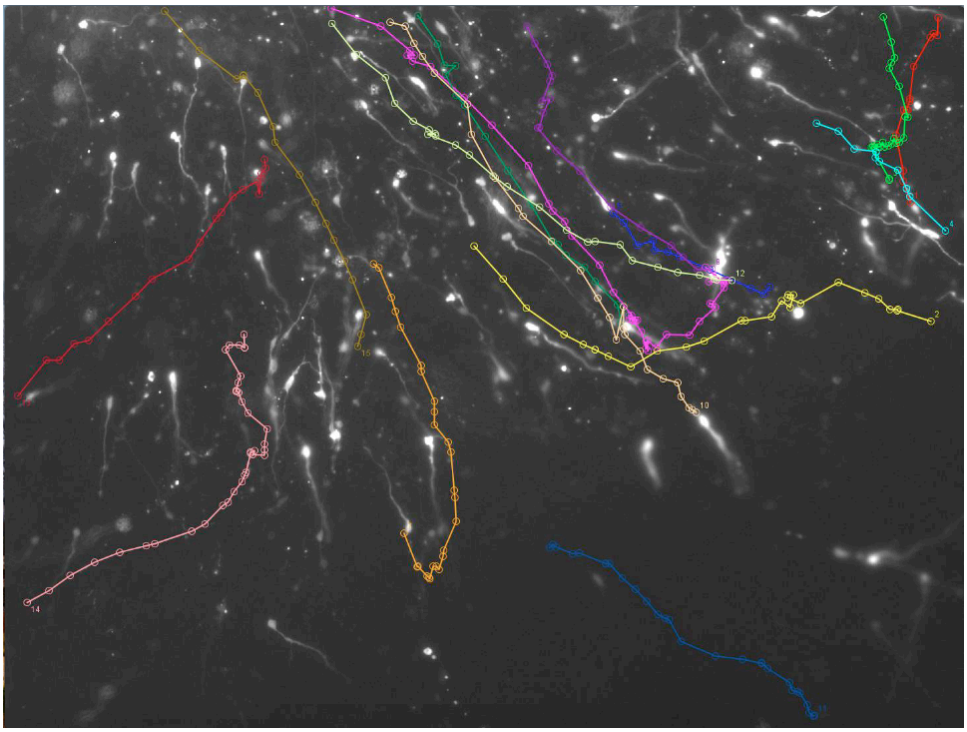

Movie 3: Tracks of migrating neurons showing turns in BPA treated slices.

The tracks show more turns compared to movie 2 (control, untreated).

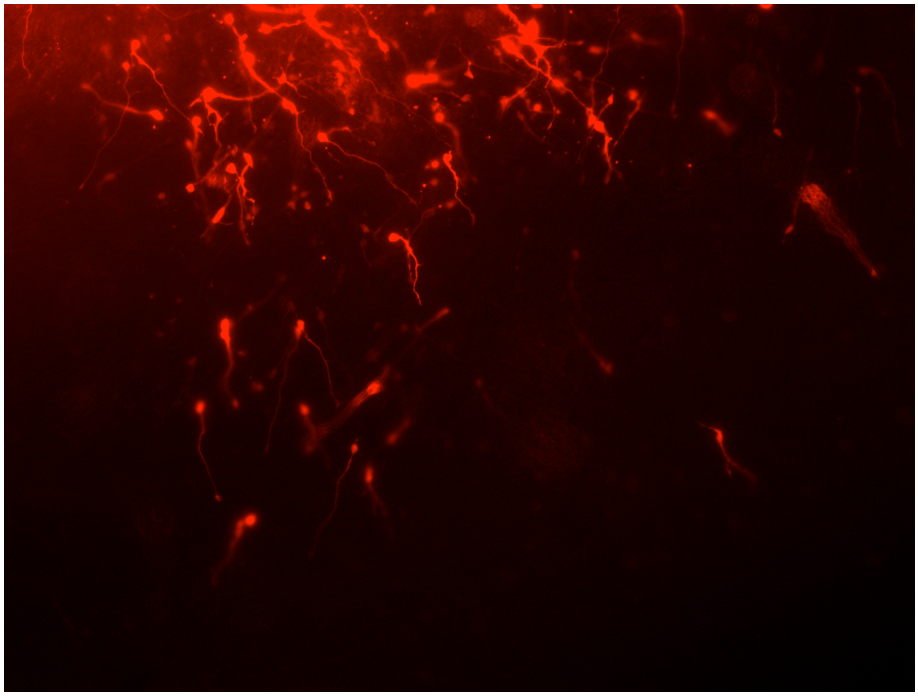

Movie 4: Migrating neurons leaving the GE in normal slices treated with KCC2 antagonist.

Neurons leaving the GE neurons and travelling towards the neocortex are guided by the leading process and display exploratory behaviors such as turning, giving out and retracting processes, changing direction and pausing.

Chapter 4: Discussion

Summary of Findings

Disruptions in neuronal migration lead to cortical dysplasia, one of the underlying causes in neurodevelopmental and psychiatric disorders including epilepsy, schizophrenia and autism spectrum disorders (ASD) (14; 23; 71; 72; 101; 109; 116). These disorders affect about 120 million people worldwide and yet have no well-defined treatment because of limitations in our understanding of the etiologies and pathogenic mechanisms of abnormal neuronal migration. Factors involve environmental toxins, injuries, genetic alterations, and infections, which all can affect brain development leading to disruptions in neuronal migration during corticogenesis. During corticogenesis, many proteins regulate the migration of GABAergic interneurons from the GE to their destination in the cortex (54; 77; 83; 110). Dysregulation of any of these proteins can result in abnormal migration behavior. NKCC1 and the KCC2 are chloride channels, which mediate the activity of GABAergic networks by regulating the intracellular chloride concentration. The developmental regulation of NKCC1 and KCC2 expression changes GABAergic network activity from depolarizing (excitatory) in immature neurons to hyperpolarizing (inhibitory) in mature neurons (77). During late embryonic and early postnatal life, the increased expression of the chloride importer (NKCC1) over the chloride exporter (KCC2) in immature neurons maintains a high intracellular Cl^- concentration, which makes GABAergic networks depolarizing (35). On maturation, KCC2 expression increases whereas NKCC1 expression decreases to maintain a low intracellular Cl^- concentration making GABA induced currents hyperpolarizing. This functional switch plays an important role in regulating the migration of interneurons to their appropriate destination in the cortex (24). Manipulation of KCC2 during development of the neocortex, therefore, could elucidate the role of this ion channel protein during neuronal migration.

In earlier studies, our group produced a model of cortical dysplasia in the ferret by administering MAM on E33. We found a precocious upregulation of KCC2 in this model at P0 that correlated with decreased speed of interneurons moving toward the neocortex and alterations in other features of migration (3). Building on this previous work, the first part of our current study seeks to define the pattern of KCC2 expression, its cellular localization and colocalization with other neuronal markers in the neocortex of normal and MAM treated ferrets. Our findings show that E33 MAM treatment increases KCC2 protein expression at P0, P7, P14 and P35. Regarding the pattern of expression, we find that KCC2 is initially high in the subplate at P0 and P7 and then distributes evenly through the cortical layers at P14 and P35 in both normal and MAM treated ferret cortex. We also show that KCC2 is localized in the membrane at P0, P14 and P35 and coloclalizes with calretinin expressing cells (at P0), MAP2 expressing cells (at P0 and P35) and parvalbumin expressing cells at P35 in both normal an MAM treated ferret cortex. In the second part, we investigate the effect of KCC2 manipulation on features of migrating neurons leaving the GE and coursing to the neocortex of both normal and MAM treated ferrets. Our findings show that 50nM BPA treatment downregulates KCC2 protein and this correlates with increased speed and step size of migrating neurons leaving the GE. Similarly, KCC2 inhibition with 5μM of the KCC2 antagonist (VU0240551) correlates with increased speed and step size of migrating neurons leaving the GE in both normal and MAM treated cortices.

KCC2 Expression in the Neocortex

In this study, we find KCC2 highly expressed in the subplate at P0 and P7. This age bracket in ferrets corresponds to gestational day 80-95 in Macaque monkey and 105-123 in humans (30). Bayatti and colleagues found KCC2 expression in the human subplate from pregnancy day 112, which agrees with our findings of KCC2 immunoreactivity in ferret subplate (15; 125). The presence of KCC2 in the subplate at this age in ferrets supports the role of KCC2 in the formation of synaptic networks

together with the GABAergic system in the neocortex. This differs from rodents who lack KCC2 in the subplate at the corresponding age highlighting an additional distinction in the development of gyrencephalic and lissencephalic brains (126). We also find calretinin positive cells colocalize with KCC2 expressing cells in the subplate. Our earlier studies in developing ferrets also report that delivery of MAM on E33 results in increased levels of $GABA_AR$s and altered functional properties in neurons migrating from the GE (1). These findings strengthen the assertion that KCC2 plays a role in the formation of the interneuron synaptic networks during brain development.

Existing data identify KCC2 as a membrane protein (22; 29; 85; 94) but the KCC2 immunostaining in ferret neocortex in our work was not definite on that score. Our results from western blots of extracted membrane proteins and concomitant cytosolic protein show that KCC2 is localized in the membrane fraction of our sample and absent in the cytosolic fraction at P0, P14 and P35, which agrees with previous findings. KCC2 localization in the cell membrane makes sense because it is an ion channel and functionally expected to be a membrane protein. KCC2 colocalizes with MAP2 expressing neurons in the ferret at P0 and P35 and also with calretinin (CR) expressing cells at P0 and parvalbumin (PV) expressing cells at P35. While MAP2 is a general neuronal marker including both excitatory and inhibitory neurons, CR and PV are markers for inhibitory interneurons. KCC2 colocalizing with CR and PV indicate its close association and working relationship with the GABAergic system. Colocalization with MAP2 indicates that KCC2 expression may occur at the postsynaptic end on excitatory neurons. This would also agree with our earlier findings reporting that after MAM treatment, recording from pyramidal cells in the mature cerebral cortex show increased amplitude of IPSCs and increased amplitude and frequency of miniature IPSCs (Abbah et al 2014). These pieces of information suggest that the levels and presence of KCC2 and $GABA_AR$ are intimately related.

KCC2 Upregulation by E33 MAM Treatment

The mechanism of KCC2 expression and regulation is well understood but understanding the endogenous mechanism that initiates and controls KCC2 upregulation during development is emerging. Given the important role of KCC2 in motogenic control and termination of neuronal migration during brain development, knowledge of the detailed mechanisms of intrinsic factors that regulate KCC2 upregulation will enhance the current understanding of neurodevelopmental disorders involving cortical dysplasia. Bortone and Polleux (2009) (24) reported that determination of the factors that regulate and alter KCC2 expression in cortical interneurons would greatly improve our understanding of the mechanisms regulating the termination of interneuron migration. Our E33 gestational MAM model shows that MAM treatment upregulates KCC2 mRNA at P0 with a corresponding KCC2 protein upregulation at P0, P7, P14 and P35 (Chapter 2). It is therefore a suitable and promising model for investigating the factors and mechanisms that regulate and alter KCC2 expression in a gyrencephalic animal. Looking into the future, our group seeks to dissect the mechanisms leading to KCC2 upregulation following MAM treatment starting investigations into possible epigenetic modifications. Although MAM is a methylating agent and a substantial amount of data show that methylation represses gene expression through the methyl CpG binding protein (MeCP2), additional evidence shows that the MeCP2 plays a dual role as both a transcriptional repressor of some genes and activator of other genes depending on the molecules recruited at the binding target (11; 28). As a transcriptional activator MeCP2 associates with cyclic adenosine monophosphate response element-binding protein1 (CREB1) at the promoter of the activated gene whereas its association with the paired amphipathic helix protein (Sin3a) characterizes transcriptional repression (28). Our investigations will therefore focus on assessment of association of KCC2 gene and the MeCP2 protein with focus on downstream pathways involving CREB1.

KCC2 Manipulation and its Effect on Neuronal Migration

The activity and/or expression of KCC2 protein during migration correlates with the speed of migrating neurons in an inverse relationship such that a higher activity and/or expression of KCC2 decreases the speed of migrating neurons and vice versa. Bortone and Polleux (2009) (24) show during migration that precocious KCC2 overexpression acts as a switch making GABA hyperpolarizing, reducing Ca^{2+} influx through the VSCCs, which significantly reduces interneuron motility. Migrating neurons integrate a balance between hyperpolarizing GABA and depolarizing glutamate signals to determine when to stop moving. A prevalence and persistence of an overall depolarizing signal opens the VSCC on nearby pyramidal neurons leading a calcium flux increasing intracellular calcium levels, which eventually stimulates the cytoskeleton for faster movement through cascades of downstream mechanisms. On the other hand a net depolarizing signal between GABA and glutamate neurons keeps the VSCC shut leading to low intracellular calcium and inhibition of neuronal motility and eventually termination of migration. Abbah and Juliano (2014) (3) also show that gestational MAM treatment upregulates KCC2 protein, which slows down migrating interneurons. Inhibition of GABA receptors following MAM treatment rescued migrating neurons from the MAM effect leading to increased migration speed.

On the other hand, Yeo et al (2013) (132) show that KCC2 downregulation delays the perinatal chloride shift leading to an increase in interneuron motility. Similarly, we show in this study that KCC2 downregulation and inhibition of KCC2 activity increase the motility of migrating interneurons. Clearly, KCC2 manipulation disrupts interneuron motility leading to a form of cortical dysplasia ultimately contributing to the pathogenesis of neurodevelopmental disorders. Although we anticipate some form of abnormalities in animals subjected to KCC2 manipulation during development, it may be useful to study the phenotype of those animals in order to translate meaningfully to human conditions. Meanwhile investigating the endogenous mechanisms involved in KCC2 expression and

regulation will be a giant leap in understanding factors influencing neuronal migration. In future studies we will investigate the downstream mechanisms that stimulate the neuronal cytoskeleton leading to increased motility following KCC2 manipulation. The calcium influx through the VSCC during neuronal migration most likely stimulates the actinomyosin cytoskeleton and microtubule filaments to increase the migration speed of neurons possibly by activating downstream cyclic AMP dependent kinase pathways (51; 56; 134).

CONCLUSION

This study provides insight into the expression pattern and localization of KCC2 in ferret neocortex. The alteration of features of migrating neurons following KCC2 manipulation within a short time period (as summarized in Figure 19) reveals that a longer prenatal impairment on KCC2 expression and/or function can have more drastic and deleterious effects on corticogenesis. The effect of exposure to environmental toxins (such as MAM and BPA) on brain development cannot be overemphasized. A developing brain is not a "miniature" adult brain and hence needs to be protected from hazardous environmental toxins. The KCC2 expression and functionary systems remain potential target to unveil the mechanisms of abnormal neuronal migration during corticogenesis and its implication in the pathogenesis of neurodevelopmental disorders such as epilepsy, schizophrenia, autism spectrum disorder and other related disorders.

Future Directions

In our future directions we will consider carrying out the following experiments:

1. Repeat live imaging experiment to increase the sample size for E33-MAM treated ferrets.
2. Investigate the mechanisms of MAM on KCC2 upregulation targeting primarily epigenetic modifications including methylation and acetylation.
3. Investigate the downstream mechanisms of stimulation of neuronal motility by KCC2 action through the voltage sensitive calcium channels.
4. Explore other forms of KCC2 manipulation such as overexpression constructs and knockdown using shRNA.

REFERENCES

1. Abbah J, Braga MF, Juliano SL. 2014. Targeted disruption of layer 4 during development increases GABAA receptor neurotransmission in the neocortex. *J Neurophysiol* 111:323-35
2. Abbah J, Juliano SL. 2013. Altered Migratory Behavior of Interneurons in a Model of Cortical Dysplasia: The Influence of Elevated GABAA Activity. *Cerebral cortex*
3. Abbah J, Juliano SL. 2014. Altered migratory behavior of interneurons in a model of cortical dysplasia: the influence of elevated GABAA activity. *Cereb Cortex* 24:2297-308
4. Adams NC, Tomoda T, Cooper M, Dietz G, Hatten ME. 2002. Mice that lack astrotactin have slowed neuronal migration. *Development* 129:965-72
5. Agez M, Schultz P, Medina I, Baker DJ, Burnham MP, et al. 2017. Molecular architecture of potassium chloride co-transporter KCC2. *Sci Rep* 7:16452
6. Anderson SA, Eisenstat DD, Shi L, Rubenstein JL. 1997. Interneuron migration from basal forebrain to neocortex: dependence on Dlx genes. *Science* 278:474-6
7. Ang ES, Jr., Haydar TF, Gluncic V, Rakic P. 2003. Four-dimensional migratory coordinates of GABAergic interneurons in the developing mouse cortex. *J Neurosci* 23:5805-15
8. Anton ES, Marchionni MA, Lee KF, Rakic P. 1997. Role of GGF/neuregulin signaling in interactions between migrating neurons and radial glia in the developing cerebral cortex. *Development* 124:3501-10
9. Aronica E, Boer K, Redeker S, Spliet WG, van Rijen PC, et al. 2007. Differential expression patterns of chloride transporters, Na+-K+-2Cl--cotransporter and K+-Cl--cotransporter, in epilepsy-associated malformations of cortical development. *Neuroscience* 145:185-96
10. Ayala R, Shu T, Tsai LH. 2007. Trekking across the brain: the journey of neuronal migration. *Cell* 128:29-43
11. Bannister AJ, Kouzarides T. 2011. Regulation of chromatin by histone modifications. *Cell Res* 21:381-95
12. Bartolini F, Andres-Delgado L, Qu X, Nik S, Ramalingam N, et al. 2016. An mDia1-INF2 formin activation cascade facilitated by IQGAP1 regulates stable microtubules in migrating cells. *Mol Biol Cell* 27:1797-808
13. Bartolini G, Ciceri G, Marin O. 2013. Integration of GABAergic interneurons into cortical cell assemblies: lessons from embryos and adults. *Neuron* 79:849-64
14. Battaglia G, Pagliardini S, Saglietti L, Cattabeni F, Di Luca M, et al. 2003. Neurogenesis in cerebral heterotopia induced in rats by prenatal methylazoxymethanol treatment. *Cereb Cortex* 13:736-48
15. Bayatti N, Moss JA, Sun L, Ambrose P, Ward JF, et al. 2008. A molecular neuroanatomical study of the developing human neocortex from 8 to 17 postconceptional weeks revealing the early differentiation of the subplate and subventricular zone. *Cereb Cortex* 18:1536-48
16. Behar TN, Li YX, Tran HT, Ma W, Dunlap V, et al. 1996. GABA stimulates chemotaxis and chemokinesis of embryonic cortical neurons via calcium-dependent mechanisms. *J Neurosci* 16:1808-18
17. Ben-Ari Y. 2014. The GABA excitatory/inhibitory developmental sequence: a personal journey. *Neuroscience* 279:187-219
18. Ben-Ari Y, Cherubini E, Corradetti R, Gaiarsa JL. 1989. Giant synaptic potentials in immature rat CA3 hippocampal neurones. *J Physiol* 416:303-25
19. Ben-Ari Y, Khalilov I, Kahle KT, Cherubini E. 2012. The GABA excitatory/inhibitory shift in brain maturation and neurological disorders. *Neuroscientist* 18:467-86

20. Bielle F, Griveau A, Narboux-Neme N, Vigneau S, Sigrist M, et al. 2005. Multiple origins of Cajal-Retzius cells at the borders of the developing pallium. *Nat Neurosci* 8:1002-12
21. Biwersi J, Verkman AS. 1991. Cell-permeable fluorescent indicator for cytosolic chloride. *Biochemistry* 30:7879-83
22. Blaesse P, Airaksinen MS, Rivera C, Kaila K. 2009. Cation-chloride cotransporters and neuronal function. *Neuron* 61:820-38
23. Blumcke I, Vinters HV, Armstrong D, Aronica E, Thom M, Spreafico R. 2009. Malformations of cortical development and epilepsies: neuropathological findings with emphasis on focal cortical dysplasia. *Epileptic Disord* 11:181-93
24. Bortone D, Polleux F. 2009. KCC2 expression promotes the termination of cortical interneuron migration in a voltage-sensitive calcium-dependent manner. *Neuron* 62:53-71
25. Cabaton NJ, Wadia PR, Rubin BS, Zalko D, Schaeberle CM, et al. 2011. Perinatal exposure to environmentally relevant levels of bisphenol A decreases fertility and fecundity in CD-1 mice. *Environ Health Perspect* 119:547-52
26. Cancedda L, Fiumelli H, Chen K, Poo MM. 2007. Excitatory GABA action is essential for morphological maturation of cortical neurons in vivo. *J Neurosci* 27:5224-35
27. Cattaneo E, Reinach B, Caputi A, Cattabeni F, Di Luca M. 1995. Selective in vitro blockade of neuroepithelial cells proliferation by methylazoxymethanol, a molecule capable of inducing long lasting functional impairments. *J Neurosci Res* 41:640-7
28. Chahrour M, Jung SY, Shaw C, Zhou X, Wong ST, et al. 2008. MeCP2, a key contributor to neurological disease, activates and represses transcription. *Science* 320:1224-9
29. Chamma I, Chevy Q, Poncer JC, Levi S. 2012. Role of the neuronal K-Cl co-transporter KCC2 in inhibitory and excitatory neurotransmission. *Front Cell Neurosci* 6:5
30. Clancy B, Darlington RB, Finlay BL. 2001. Translating developmental time across mammalian species. *Neuroscience* 105:7-17
31. Cobos I, Calcagnotto ME, Vilaythong AJ, Thwin MT, Noebels JL, et al. 2005. Mice lacking Dlx1 show subtype-specific loss of interneurons, reduced inhibition and epilepsy. *Nat Neurosci* 8:1059-68
32. Cuzon VC, Yeh PW, Cheng Q, Yeh HH. 2006. Ambient GABA promotes cortical entry of tangentially migrating cells derived from the medial ganglionic eminence. *Cereb Cortex* 16:1377-88
33. DeFelipe J, Lopez-Cruz PL, Benavides-Piccione R, Bielza C, Larranaga P, et al. 2013. New insights into the classification and nomenclature of cortical GABAergic interneurons. *Nat Rev Neurosci* 14:202-16
34. Deisz RA, Wierschke S, Schneider UC, Dehnicke C. 2014. Effects of VU0240551, a novel KCC2 antagonist, and DIDS on chloride homeostasis of neocortical neurons from rats and humans. *Neuroscience* 277:831-41
35. Delpire E. 2000. Cation-Chloride Cotransporters in Neuronal Communication. *News in physiological sciences : an international journal of physiology produced jointly by the International Union of Physiological Sciences and the American Physiological Society* 15:309-12
36. Delpire E, Days E, Lewis LM, Mi D, Kim K, et al. 2009. Small-molecule screen identifies inhibitors of the neuronal K-Cl cotransporter KCC2. *Proc Natl Acad Sci U S A* 106:5383-8
37. Dickson BJ. 2002. Molecular mechanisms of axon guidance. *Science* 298:1959-64
38. Dillon N. 2006. Gene regulation and large-scale chromatin organization in the nucleus. *Chromosome Res* 14:117-26

39. Esclaire F, Kisby G, Spencer P, Milne J, Lesort M, Hugon J. 1999. The Guam cycad toxin methylazoxymethanol damages neuronal DNA and modulates tau mRNA expression and excitotoxicity. *Experimental neurology* 155:11-21
40. Fietz SA, Kelava I, Vogt J, Wilsch-Brauninger M, Stenzel D, et al. 2010. OSVZ progenitors of human and ferret neocortex are epithelial-like and expand by integrin signaling. *Nat Neurosci* 13:690-9
41. Fishell G, Hatten ME. 1991. Astrotactin provides a receptor system for CNS neuronal migration. *Development* 113:755-65
42. Fishell G, Kriegstein A. 2005. Cortical development: new concepts. *Neuron* 46:361-2
43. Flames N, Long JE, Garratt AN, Fischer TM, Gassmann M, et al. 2004. Short- and long-range attraction of cortical GABAergic interneurons by neuregulin-1. *Neuron* 44:251-61
44. Fuerst PG, Koizumi A, Masland RH, Burgess RW. 2008. Neurite arborization and mosaic spacing in the mouse retina require DSCAM. *Nature* 451:470-4
45. Gal JS, Morozov YM, Ayoub AE, Chatterjee M, Rakic P, Haydar TF. 2006. Molecular and morphological heterogeneity of neural precursors in the mouse neocortical proliferative zones. *J Neurosci* 26:1045-56
46. Ganguly K, Schinder AF, Wong ST, Poo M. 2001. GABA itself promotes the developmental switch of neuronal GABAergic responses from excitation to inhibition. *Cell* 105:521-32
47. Gauvain G, Chamma I, Chevy Q, Cabezas C, Irinopoulou T, et al. 2011. The neuronal K-Cl cotransporter KCC2 influences postsynaptic AMPA receptor content and lateral diffusion in dendritic spines. *Proceedings of the National Academy of Sciences of the United States of America* 108:15474-9
48. Gelman DM, Marin O. 2010. Generation of interneuron diversity in the mouse cerebral cortex. *Eur J Neurosci* 31:2136-41
49. Gertz CC, Lui JH, LaMonica BE, Wang X, Kriegstein AR. 2014. Diverse behaviors of outer radial glia in developing ferret and human cortex. *J Neurosci* 34:2559-70
50. Golub MS, Wu KL, Kaufman FL, Li LH, Moran-Messen F, et al. 2010. Bisphenol A: developmental toxicity from early prenatal exposure. *Birth Defects Res B Dev Reprod Toxicol* 89:441-66
51. Gomez TM, Zheng JQ. 2006. The molecular basis for calcium-dependent axon pathfinding. *Nat Rev Neurosci* 7:115-25
52. Gulyas AI, Sik A, Payne JA, Kaila K, Freund TF. 2001. The KCl cotransporter, KCC2, is highly expressed in the vicinity of excitatory synapses in the rat hippocampus. *Eur J Neurosci* 13:2205-17
53. Gupta A, Tsai LH, Wynshaw-Boris A. 2002. Life is a journey: a genetic look at neocortical development. *Nat Rev Genet* 3:342-55
54. Hatten ME. 2002. New directions in neuronal migration. *Science* 297:1660-3
55. Heck N, Kilb W, Reiprich P, Kubota H, Furukawa T, et al. 2007. GABA-A receptors regulate neocortical neuronal migration in vitro and in vivo. *Cereb Cortex* 17:138-48
56. Henley J, Poo MM. 2004. Guiding neuronal growth cones using Ca2+ signals. *Trends Cell Biol* 14:320-30
57. Howell BW, Herrick TM, Cooper JA. 1999. Reelin-induced tyrosine [corrected] phosphorylation of disabled 1 during neuronal positioning. *Genes Dev* 13:643-8
58. Inglefield JR, Schwartz-Bloom RD. 1999. Fluorescence imaging of changes in intracellular chloride in living brain slices. *Methods* 18:197-203
59. Itoh K, Yaoi T, Fushiki S. 2012. Bisphenol A, an endocrine-disrupting chemical, and brain development. *Neuropathology* 32:447-57

60. Jablonska B. 2004. GABAA Receptors Reorganize when Layer 4 in Ferret Somatosensory Cortex is Disrupted by Methylazoxymethanol (MAM). *Cerebral Cortex* 14:432-40
61. Jablonska BALS, A. L., Sidney L. Palmer, S. L, Noctor, S. C and Juliano, S. L. 2004. GABAA Receptors Reorganize when Layer 4 in Ferret Somatosensory Cortex is Disrupted by Methylazoxymethanol (MAM). *Cerebral Cortex* 14:432-40
62. Jackson CA, Peduzzi JD, Hickey TL. 1989. Visual cortex development in the ferret. I. Genesis and migration of visual cortical neurons. *J Neurosci* 9:1242-53
63. Jaenisch N, Witte OW, Frahm C. 2010. Downregulation of potassium chloride cotransporter KCC2 after transient focal cerebral ischemia. *Stroke* 41:e151-9
64. Johnston MV, Coyle JT. 1979. Histological and neurochemical effects of fetal treatment with methylazoxymethanol on rat neocortex in adulthood. *Brain Res* 170:135-55
65. Kahle KT, Staley KJ, Nahed BV, Gamba G, Hebert SC, et al. 2008. Roles of the cation-chloride cotransporters in neurological disease. *Nat Clin Pract Neurol* 4:490-503
66. Kappeler C, Saillour Y, Baudoin JP, Tuy FP, Alvarez C, et al. 2006. Branching and nucleokinesis defects in migrating interneurons derived from doublecortin knockout mice. *Hum Mol Genet* 15:1387-400
67. Komada M, Asai Y, Morii M, Matsuki M, Sato M, Nagao T. 2012. Maternal bisphenol A oral dosing relates to the acceleration of neurogenesis in the developing neocortex of mouse fetuses. *Toxicology* 295:31-8
68. Komada M, Itoh S, Kawachi K, Kagawa N, Ikeda Y, Nagao T. 2014. Newborn mice exposed prenatally to bisphenol A show hyperactivity and defective neocortical development. *Toxicology* 323:51-60
69. Kostovic I, Rakic P. 1990. Developmental history of the transient subplate zone in the visual and somatosensory cortex of the macaque monkey and human brain. *J Comp Neurol* 297:441-70
70. Krapf R, Berry CA, Verkman AS. 1988. Estimation of intracellular chloride activity in isolated perfused rabbit proximal convoluted tubules using a fluorescent indicator. *Biophys J* 53:955-62
71. Levy LM, Degnan AJ. 2013. GABA-based evaluation of neurologic conditions: MR spectroscopy. *AJNR Am J Neuroradiol* 34:259-65
72. Lewis DA. 2000. GABAergic local circuit neurons and prefrontal cortical dysfunction in schizophrenia. *Brain Res Brain Res Rev* 31:270-6
73. Li H, Khirug S, Cai C, Ludwig A, Blaesse P, et al. 2007. KCC2 interacts with the dendritic cytoskeleton to promote spine development. *Neuron* 56:1019-33
74. Liu Z, Neff RA, Berg DK. 2006. Sequential interplay of nicotinic and GABAergic signaling guides neuronal development. *Science* 314:1610-3
75. Llano O, Smirnov S, Soni S, Golubtsov A, Guillemin I, et al. 2015. KCC2 regulates actin dynamics in dendritic spines via interaction with beta-PIX. *J Cell Biol* 209:671-86
76. Lopez-Bendito G, Cautinat A, Sanchez JA, Bielle F, Flames N, et al. 2006. Tangential neuronal migration controls axon guidance: a role for neuregulin-1 in thalamocortical axon navigation. *Cell* 125:127-42
77. Lu J, Karadsheh M, Delpire E. 1999. Developmental regulation of the neuronal-specific isoform of K-Cl cotransporter KCC2 in postnatal rat brains. *J Neurobiol* 39:558-68
78. Ludwig A, Uvarov P, Soni S, Thomas-Crusells J, Airaksinen MS, Rivera C. 2011. Early growth response 4 mediates BDNF induction of potassium chloride cotransporter 2 transcription. *J Neurosci* 31:644-9

79. Marin O. 2003. Directional guidance of interneuron migration to the cerebral cortex relies on subcortical Slit1/2-independent repulsion and cortical attraction. *Development* 130:1889-901
80. Marin O, Rubenstein JL. 2001. A long, remarkable journey: tangential migration in the telencephalon. *Nat Rev Neurosci* 2:780-90
81. Marin O, Rubenstein JL. 2003. Cell migration in the forebrain. *Annu Rev Neurosci* 26:441-83
82. Marin O, Valdeolmillos M, Moya F. 2006. Neurons in motion: same principles for different shapes? *Trends Neurosci* 29:655-61
83. Marin O, Valiente M, Ge X, Tsai LH. 2010. Guiding neuronal cell migrations. *Cold Spring Harb Perspect Biol* 2:a001834
84. McLaughlin DF, Juliano SL. 2005. Disruption of layer 4 development alters laminar processing in ferret somatosensory cortex. *Cereb Cortex* 15:1791-803
85. Medina I, Friedel P, Rivera C, Kahle KT, Kourdougli N, et al. 2014. Current view on the functional regulation of the neuronal K(+)-Cl(-) cotransporter KCC2. *Front Cell Neurosci* 8:27
86. Miyoshi G, Fishell G. 2011. GABAergic interneuron lineages selectively sort into specific cortical layers during early postnatal development. *Cereb Cortex* 21:845-52
87. Mueller AL, Taube JS, Schwartzkroin PA. 1984. Development of hyperpolarizing inhibitory postsynaptic potentials and hyperpolarizing response to gamma-aminobutyric acid in rabbit hippocampus studied in vitro. *J Neurosci* 4:860-7
88. Nakagami A, Negishi T, Kawasaki K, Imai N, Nishida Y, et al. 2009. Alterations in male infant behaviors towards its mother by prenatal exposure to bisphenol A in cynomolgus monkeys (Macaca fascicularis) during early suckling period. *Psychoneuroendocrinology* 34:1189-97
89. Nasrallah IM, McManus MF, Pancoast MM, Wynshaw-Boris A, Golden JA. 2006. Analysis of non-radial interneuron migration dynamics and its disruption in Lis1+/- mice. *J Comp Neurol* 496:847-58
90. Negri-Cesi P. 2015. Bisphenol A Interaction With Brain Development and Functions. *Dose Response* 13:1559325815590394
91. Noctor SC, Palmer SL, McLaughlin DF, Juliano SL. 2001. Disruption of layers 3 and 4 during development results in altered thalamocortical projections in ferret somatosensory cortex. *J Neurosci* 21:3184-95
92. Noctor SC, Scholnicoff NJ, Juliano SL. 1997. Histogenesis of ferret somatosensory cortex. *J Comp Neurol* 387:179-93
93. Palmer SL, Noctor SC, Jablonska B, Juliano SL. 2001. Laminar specific alterations of thalamocortical projections in organotypic cultures following layer 4 disruption in ferret somatosensory cortex. *Eur J Neurosci* 13:1559-71
94. Payne JA, Stevenson TJ, Donaldson LF. 1996. Molecular characterization of a putative K-Cl cotransporter in rat brain. A neuronal-specific isoform. *J Biol Chem* 271:16245-52
95. Polleux F, Whitford KL, Dijkhuizen PA, Vitalis T, Ghosh A. 2002. Control of cortical interneuron migration by neurotrophins and PI3-kinase signaling. *Development* 129:3147-60
96. Poluch S, Drian MJ, Durand M, Astier C, Benyamin Y, Konig N. 2001. AMPA receptor activation leads to neurite retraction in tangentially migrating neurons in the intermediate zone of the embryonic rat neocortex. *Journal of neuroscience research* 63:35-44
97. Poluch S, Jablonska B, Juliano SL. 2008. Alteration of interneuron migration in a ferret model of cortical dysplasia. *Cerebral cortex* 18:78-92
98. Poluch S, Juliano SL. 2007. A normal radial glial scaffold is necessary for migration of interneurons during neocortical development. *Glia* 55:822-30

99. Poluch S, Juliano SL. 2015. Fine-tuning of neurogenesis is essential for the evolutionary expansion of the cerebral cortex. *Cereb Cortex* 25:346-64
100. Poluch S, Rossel M, Konig N. 2003. AMPA-evoked ion influx is strongest in tangential neurons of the rat neocortical intermediate zone close to the front of the migratory stream. *Dev Dyn* 227:416-21
101. Powell EM, Campbell DB, Stanwood GD, Davis C, Noebels JL, Levitt P. 2003. Genetic disruption of cortical interneuron development causes region- and GABA cell type-specific deficits, epilepsy, and behavioral dysfunction. *J Neurosci* 23:622-31
102. Puskarjov M, Ahmad F, Kaila K, Blaesse P. 2012. Activity-dependent cleavage of the K-Cl cotransporter KCC2 mediated by calcium-activated protease calpain. *J Neurosci* 32:11356-64
103. Rakic P. 1974. Neurons in rhesus monkey visual cortex: systematic relation between time of origin and eventual disposition. *Science* 183:425-7
104. Rakic P. 1990. Principles of neural cell migration. *Experientia* 46:882-91
105. Rakic P. 2007. The radial edifice of cortical architecture: from neuronal silhouettes to genetic engineering. *Brain Res Rev* 55:204-19
106. Rakic P. 2009. Evolution of the neocortex: a perspective from developmental biology. *Nat Rev Neurosci* 10:724-35
107. Rivera C, Li H, Thomas-Crusells J, Lahtinen H, Viitanen T, et al. 2002. BDNF-induced TrkB activation down-regulates the K+-Cl- cotransporter KCC2 and impairs neuronal Cl- extrusion. *J Cell Biol* 159:747-52
108. Rivera C, Voipio J, Thomas-Crusells J, Li H, Emri Z, et al. 2004. Mechanism of activity-dependent downregulation of the neuron-specific K-Cl cotransporter KCC2. *J Neurosci* 24:4683-91
109. Rubenstein JL, Merzenich MM. 2003. Model of autism: increased ratio of excitation/inhibition in key neural systems. *Genes Brain Behav* 2:255-67
110. Rudolph J, Zimmer G, Steinecke A, Barchmann S, Bolz J. 2010. Ephrins guide migrating cortical interneurons in the basal telencephalon. *Cell Adhesion & Migration* 4:400-8
111. Rudolph J, Zimmer G, Steinecke A, Barchmann S, Bolz J. 2014. Ephrins guide migrating cortical interneurons in the basal telencephalon. *Cell Adhesion & Migration* 4:400-8
112. Rudy B, Fishell G, Lee S, Hjerling-Leffler J. 2011. Three groups of interneurons account for nearly 100% of neocortical GABAergic neurons. *Dev Neurobiol* 71:45-61
113. Schwartz RD, Yu X. 1995. Optical imaging of intracellular chloride in living brain slices. *J Neurosci Methods* 62:185-92
114. Takiguchi-Hayashi K, Sekiguchi M, Ashigaki S, Takamatsu M, Hasegawa H, et al. 2004. Generation of reelin-positive marginal zone cells from the caudomedial wall of telencephalic vesicles. *J Neurosci* 24:2286-95
115. Tanaka D, Nakaya Y, Yanagawa Y, Obata K, Murakami F. 2003. Multimodal tangential migration of neocortical GABAergic neurons independent of GPI-anchored proteins. *Development* 130:5803-13
116. Tassi L, Colombo N, Garbelli R, Francione S, Lo Russo G, et al. 2002. Focal cortical dysplasia: neuropathological subtypes, EEG, neuroimaging and surgical outcome. *Brain* 125:1719-32
117. Tessier-Lavigne M, Goodman CS. 1996. The molecular biology of axon guidance. *Science* 274:1123-33
118. Uvarov P, Ludwig A, Markkanen M, Rivera C, Airaksinen MS. 2006. Upregulation of the neuron-specific K+/Cl- cotransporter expression by transcription factor early growth response 4. *J Neurosci* 26:13463-73
119. Valiente M, Marin O. 2010. Neuronal migration mechanisms in development and disease. *Curr Opin Neurobiol* 20:68-78

120. Verkman AS. 1990. Development and biological applications of chloride-sensitive fluorescent indicators. *Am J Physiol* 259:C375-88
121. Vom Saal FS, Nagel SC, Coe BL, Angle BM, Taylor JA. 2012. The estrogenic endocrine disrupting chemical bisphenol A (BPA) and obesity. *Mol Cell Endocrinol* 354:74-84
122. Wang C, Shimizu-Okabe C, Watanabe K, Okabe A, Matsuzaki H, et al. 2002. Developmental changes in KCC1, KCC2, and NKCC1 mRNA expressions in the rat brain. *Brain Res Dev Brain Res* 139:59-66
123. Wang DD, Kriegstein AR. 2008. GABA regulates excitatory synapse formation in the neocortex via NMDA receptor activation. *J Neurosci* 28:5547-58
124. Wang DD, Kriegstein AR. 2009. Defining the role of GABA in cortical development. *J Physiol* 587:1873-9
125. Wang WZ, Hoerder-Suabedissen A, Oeschger FM, Bayatti N, Ip BK, et al. 2010. Subplate in the developing cortex of mouse and human. *J Anat* 217:368-80
126. Watanabe M, Fukuda A. 2015. Development and regulation of chloride homeostasis in the central nervous system. *Front Cell Neurosci* 9:371
127. Welagen J, Anderson S. 2011. Origins of neocortical interneurons in mice. *Dev Neurobiol* 71:10-7
128. Whim MD, Moss GW. 2001. A novel technique that measures peptide secretion on a millisecond timescale reveals rapid changes in release. *Neuron* 30:37-50
129. Williams JR, Sharp JW, Kumari VG, Wilson M, Payne JA. 1999. The neuron-specific K-Cl cotransporter, KCC2. Antibody development and initial characterization of the protein. *The Journal of biological chemistry* 274:12656-64
130. Yee KT, Simon HH, Tessier-Lavigne M, O'Leary DM. 1999. Extension of long leading processes and neuronal migration in the mammalian brain directed by the chemoattractant netrin-1. *Neuron* 24:607-22
131. Yeo M, Berglund K, Augustine G, Liedtke W. 2009. Novel repression of Kcc2 transcription by REST-RE-1 controls developmental switch in neuronal chloride. *J Neurosci* 29:14652-62
132. Yeo M, Berglund K, Hanna M, Guo JU, Kittur J, et al. 2013. Bisphenol A delays the perinatal chloride shift in cortical neurons by epigenetic effects on the Kcc2 promoter. *Proc Natl Acad Sci U S A* 110:4315-20
133. Yoshida M, Assimacopoulos S, Jones KR, Grove EA. 2006. Massive loss of Cajal-Retzius cells does not disrupt neocortical layer order. *Development* 133:537-45
134. Zheng JQ, Poo MM. 2007. Calcium signaling in neuronal motility. *Annu Rev Cell Dev Biol* 23:375-404